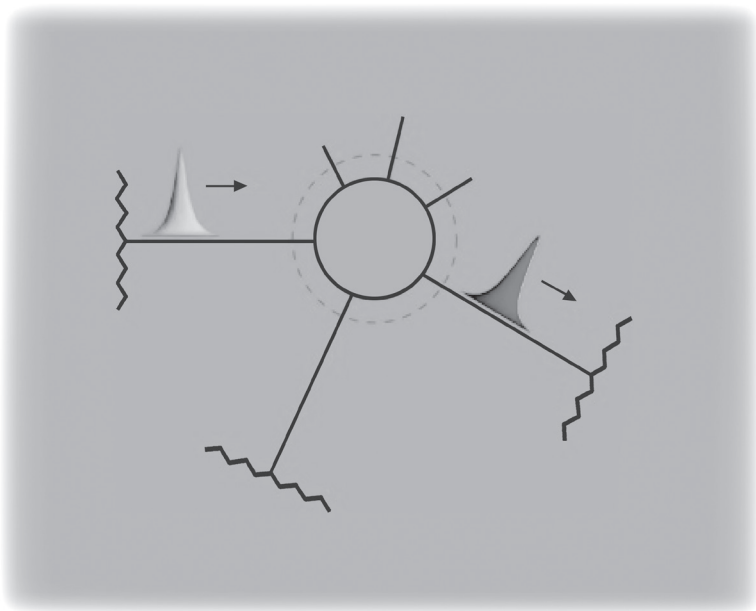


Scattering Matrix Approach to Non-Stationary Quantum Transport



Michael V Moskalets

National Technical University, "Kharkiv Polytechnical Institute", Ukraine

Published by

Imperial College Press
57 Shelton Street
Covent Garden
London WC2H 9HE

Distributed by

World Scientific Publishing Co. Pte. Ltd.
5 Toh Tuck Link, Singapore 596224
USA office: 27 Warren Street, Suite 401-402, Hackensack, NJ 07601
UK office: 57 Shelton Street, Covent Garden, London WC2H 9HE

British Library Cataloguing-in-Publication Data

A catalogue record for this book is available from the British Library.

**SCATTERING MATRIX APPROACH TO NON-STATIONARY
QUANTUM TRANSPORT**

Copyright © 2012 by Imperial College Press

All rights reserved. This book, or parts thereof, may not be reproduced in any form or by any means, electronic or mechanical, including photocopying, recording or any information storage and retrieval system now known or to be invented, without written permission from the Publisher.

For photocopying of material in this volume, please pay a copying fee through the Copyright Clearance Center, Inc., 222 Rosewood Drive, Danvers, MA 01923, USA. In this case permission to photocopy is not required from the publisher.

ISBN-13 978-1-84816-834-3
ISBN-10 1-84816-834-9

Printed in Singapore.

I dedicate this book to my parents,
Anna A. Tarasenko and Vasyliy T. Moskalets

Preface

The lectures of Professor Michael Moskalets introduce basic concepts of the scattering approach to transport phenomena in time-dependent, dynamic quantum systems. For stationary problems scattering theory has been widely and successfully used to discuss electronic transport in structures so small that interference effects become important. Such systems are central to nanophysics and mesoscopic physics. The lectures extend this approach to time-dependent scatterers.

Scattering theory derives its success from two sources. The approach captures essential aspects of real experiments and is therefore useful in the laboratory. Scattering theory is often referred to as a formalism but this is almost a misnomer. In the realm of theories, the scattering approach has the advantage that it appeals to our intuition. It is an approach that is clearly not reserved only for physicists with a theoretical inclination.

The lectures provide an introduction to the stationary scattering theory and then bring the reader to the forefront of current research in the transport theory of time-dependent scatterers. Of interest are the charge and heat currents and the noise properties of such systems. Important examples are quantum pumps and mesoscopic capacitors subject to time-dependent potentials.

The lectures are clearly structured and focus on the principal points in the theoretical development. The author is didactical. The lectures develop all the mathematical steps and also provide a physically clear and transparent description of processes in dynamic nanoscopic and mesoscopic systems. The lectures present an excellent record of the current state of the field. This makes these lectures useful not only to students but also to advanced researchers.

Markus Büttiker

Acknowledgments

I am very grateful to Markus Büttiker. Without a collaboration with him that has lasted more than a decade, without numerous discussions with him, without his constant support and encouragement this book would not have been written.

I would like to thank the people with whom I directly collaborate, especially, Liliana Arrachea, Janine Splettstößer and Peter Samuelsson. The many interesting and exciting results that we found together are presented in this book. I also have to thank many people from the department of metal and semiconductor physics of the National Technical University “Kharkiv Polytechnical Institute”, Kharkiv, Ukraine, where I work, and from the department of theoretical physics of the University of Geneva, Geneva, Switzerland, which I visited many times while working on this book, for numerous useful and stimulating discussions.

And last but not least, I am very grateful to my wife Natasha for patience, support, and understanding.

Contents

<i>Preface</i>	vii
<i>Acknowledgments</i>	ix
<i>List of Figures</i>	xv
1. Landauer–Büttiker formalism	1
1.1 Scattering matrix	1
1.1.1 Scattering matrix properties	4
1.2 Current operator	9
1.3 Direct current and the distribution function	14
1.3.1 Conservation of a direct current	16
1.3.2 Difference of potentials	18
1.3.3 Difference of temperatures	20
1.4 Examples	21
1.4.1 Scattering matrix 1×1	21
1.4.2 Scattering matrix 2×2	22
1.4.3 Scattering matrix 3×3	23
1.4.4 Scatterer with two leads	25
1.4.5 Scatterer with a potential contact	28
1.4.6 Scatterer embedded in a ring	29
2. Current noise	35
2.1 Nature of a current noise	36
2.1.1 Thermal noise	37
2.1.2 Shot noise	39
2.1.3 Combined noise	40

2.2	Sample with continuous spectrum	46
2.2.1	Current correlator	47
2.2.2	Current correlator in the frequency domain	49
2.2.3	Spectral noise power for energy-independent scattering	55
2.2.4	Zero frequency noise power	56
2.2.5	Fano factor	62
3.	Non-stationary scattering theory	63
3.1	Schrödinger equation with a potential periodic in time	63
3.1.1	Perturbation theory	64
3.1.2	Floquet functions method	67
3.1.3	Potential oscillating in time and uniform in space	70
3.2	Floquet scattering matrix	71
3.2.1	Floquet scattering matrix properties	72
3.3	Current operator	73
3.3.1	Alternating current	75
3.3.2	Direct current	75
3.4	Adiabatic approximation for the Floquet scattering matrix	77
3.4.1	Frozen scattering matrix	78
3.4.2	Zeroth-order approximation	78
3.4.3	First-order approximation	79
3.5	Beyond the adiabatic approximation	83
3.5.1	Scattering matrix in mixed energy-time representation	83
3.5.2	Dynamic point-like potential	86
3.5.3	Dynamic double-barrier potential	93
3.5.4	Unitarity and the sum over trajectories	104
3.5.5	Current and the sum over trajectories	106
4.	Direct current generated by the dynamic scatterer	111
4.1	Steady particle flow	112
4.1.1	Distribution function	112
4.1.2	Adiabatic regime: Current linear in the pump frequency	114
4.1.3	Current quadratic in the pump frequency	121

4.2	Quantum pump effect	122
4.2.1	Quasi-particle picture of direct current generation	122
4.2.2	Interference mechanism of direct current generation	123
4.3	Single-parameter adiabatic direct current generation	126
5.	Alternating current generated by the dynamic scatterer	129
5.1	Adiabatic alternating current	129
5.2	External AC bias	133
5.2.1	Second quantization operators for incident and scattered electrons	136
5.2.2	Alternating current	140
5.2.3	Direct current	141
5.2.4	Adiabatic direct current	142
6.	Noise generated by the dynamic scatterer	147
6.1	Spectral noise power	147
6.2	Zero frequency spectral noise power	154
6.3	Noise in the adiabatic regime	157
6.3.1	Thermal noise	157
6.3.2	Low-temperature shot noise	158
6.3.3	High-temperature shot noise	160
6.3.4	Shot noise within a wide temperature range	161
6.3.5	Noise as a function of the pump frequency	162
7.	Energetics of a dynamic scatterer	165
7.1	DC heat current	165
7.1.1	Heat generation by the dynamic scatterer	168
7.1.2	Heat transfer between the reservoirs	168
7.2	Heat flows in the adiabatic regime	171
7.2.1	High temperatures	171
7.2.2	Low temperatures	173
8.	Dynamic mesoscopic capacitor	175
8.1	General theory for a single-channel scatterer	175
8.1.1	Scattering amplitudes	176
8.1.2	Unitarity conditions	176

8.1.3	Time-dependent current	178
8.1.4	Dissipation	179
8.1.5	Dissipation versus squared current	180
8.2	Chiral single-channel capacitor	181
8.2.1	Model and scattering amplitude	182
8.2.2	Unitarity	185
8.2.3	Gauge invariance	186
8.2.4	Time-dependent current	189
8.2.5	High-temperature current	191
8.2.6	Linear response regime	192
8.2.7	Non-linear low-frequency regime	196
8.2.8	Transient current caused by a step potential	198
9.	Quantum circuits with mesoscopic capacitor as a particle emitter	207
9.1	Quantized emission regime	207
9.1.1	Simple model for a single-particle state emitted by an adiabatic capacitor	211
9.2	Shot noise quantization	212
9.2.1	Probability interpretation of the shot noise	214
9.3	Two-particle source	216
9.3.1	Scattering amplitude	216
9.3.2	Adiabatic approximation	216
9.3.3	Mean square current	218
9.3.4	Shot noise of a two-particle source	226
9.4	Mesoscopic electron collider	229
9.4.1	Shot noise suppression	231
9.4.2	Probability analysis	234
9.5	Noisy mesoscopic electron collider	237
9.5.1	Current cross-correlator suppression	238
9.5.2	Probability analysis	240
9.6	Two-particle interference effect	243
9.6.1	Model and definitions	243
9.6.2	Scattering matrix elements	248
9.6.3	Current cross-correlator	250
	<i>Bibliography</i>	261
	<i>Index</i>	277

List of Figures

1.1	A mesoscopic sample with scattering matrix \hat{S} . The index $\alpha = 1, 2, \dots, N_r$ numbers electron reservoirs. The arrows directed to (from) the scatterer show a propagation direction for incident (scattered) electrons. The electron flow is calculated at the surface Σ shown as a dashed line.	10
1.2	The distribution function for electrons scattered into the contact $\alpha = 1$. The height of a step at $E = \mu_1$ is $ S_{12} ^2$. The scatterer is connected to two electron reservoirs at zero temperature, $T_1 = T_2 = 0$, and having chemical potentials μ_1 and μ_2	16
1.3	A single-channel scatterer. a is the amplitude of an incoming wave, b is the amplitude of a reflected wave. A zigzag line denotes an electron reservoir.	21
1.4	A two-channel scatterer. a_α (b_α) are the amplitudes of incoming (scattered) waves, $\alpha = 1, 2$	22
1.5	A three-channel scatterer. a_α (b_α) are amplitudes of incoming (scattered) waves, $\alpha = 1, 2, 3$	24
1.6	A mesoscopic scatterer with current carrying (1, 2) and potential (3) leads.	28
1.7	A one-dimensional ring of length L pierced by the magnetic flux Φ with embedded scatterer. A, B are amplitudes of an electron wave function, Eq. (1.78), $\phi = 2\pi\Phi/\Phi_0$	30

- 3.1 Scattering of a wave with unit amplitude onto the point-like dynamic potential barrier. The arrows show propagation directions. The labels are amplitudes of the corresponding waves: 1 is an amplitude of an incoming wave, $b_{1,n}^{(-)}$ is an amplitude of a reflected wave, $a_{1,n}^{(+)}$ is an amplitude of a transmitted wave. Only a single (n th) component of the Floquet wave function for scattered electrons is shown. 89
- 3.2 Two dynamic point-like potentials separated by a ballistic wire of length d . The arrows show propagation directions. The labels are amplitudes of the corresponding waves, see Eqs. (3.99), (3.100), and (3.106). 94
- 4.1 The non-equilibrium distribution function, $f_{\alpha}^{(out)}(E)$, for electrons scattered into the lead α at zero temperature. The step width is $\hbar\Omega_0$. The Fermi distribution function at zero temperature is shown by the dashed line. 113
- 4.2 The parameter space for the frozen scattering matrix in the case of two varying parameters, p_1 and p_2 . During one period the point $A(t)$ with coordinates $(p_1(t), p_2(t))$ follows a trajectory \mathcal{L} . \mathcal{F} stands for the surface area. The arrow indicates the direction of movement for $\varphi > 0$, see Eq. (4.9). 118
- 4.3 The creation and scattering of quasi-electron-hole pairs in a dynamic sample with two leads. Under the action of a potential that is periodic in time, $V(t) = V(t + \mathcal{T})$, an electron can absorb one or several energy quanta, $\hbar\Omega_0$. As a result it jumps from the occupied level to the non-occupied one, which can be viewed as the creation of a quasi-electron-hole pair. A quasi-electron (a dark circle) and a hole (a light circle) can leave the scattering region through the same lead (a) or through different leads (b). In the latter case a net charge is transferred from one reservoir to the other. 122
- 4.4 Photon-assisted scattering amplitudes for an electron propagating through a dynamic double-barrier. An electron can absorb (or emit) an energy quantum $\hbar\Omega_0$ interacting either with a potential $V_1(t)$ or with a potential $V_2(t)$. Therefore, the photon-induced scattering amplitude is a sum of two terms. 124

7.1 The heat flows caused by the dynamic scatterer with two contacts. $I_\alpha^{Q(gen)}$ is the generated heat flowing into the reservoir α and $I^{Q(pump)}$ is the pumped heat. The heat production rate is $I_{tot}^Q = I_1^{Q(gen)} + I_2^{Q(gen)}$ 168

8.1 The model for a single-cavity chiral quantum capacitor driven by a uniform potential $U(t)$. The dotted line denotes a QPC. The arrows indicate the direction of movement of electrons. . . 182

8.2 An equivalent electrical circuit to model the low-frequency response of a quantum capacitor. 192

8.3 The dependence of an emitted charge Q on the height U_0 of a potential step at zero temperature. The Fermi level is centered in the middle between the levels of the cavity. 204

9.1 The mesoscopic electron collider with a single-particle source in one of its branches. The cavity is connected to a linear edge state which in turn is connected to another linear edge state via the central QPC with transmission T_C . The arrows indicate the direction of movement of the electrons. The potential $U(t)$ induced by the back-gate generates an alternating current $I(t)$, which is split at the central QPC into the currents $I_1(t)$ and $I_2(t)$ flowing to the leads. 213

9.2 The model for a double-cavity chiral quantum capacitor. Each cavity is driven by the periodic potential $U_j(t) = U_j(t + \mathcal{T})$, $j = L, R$. Both cavities are connected via the corresponding QPCs with transmission T_L and T_R , respectively, to the same linear edge state. The arrows indicate the direction of movement of electrons. 217

9.3 The mesoscopic electron collider with a two-particle source in one of its branches. The double-cavity quantum capacitor is connected to the linear edge state, which in turn is connected via the central QPC with transmission T_C to another linear edge state. The arrows indicate the direction of movement of the electrons. The potentials $U_L(t)$ and $U_R(t)$ induced by the back-gates generate an alternating current $I(t)$, which is split at the central QPC into the currents $I_1(t)$ and $I_2(t)$ flowing to the leads. 227

9.4 The mesoscopic electron collider with single-particle sources in each of its branches. The two quantum capacitors are connected to the different linear edge states, which in turn are connected together via the central QPC with transmission T_C . The arrows indicate the direction of movement of electrons. The potentials $U_L(t)$ and $U_R(t)$ induced by the back-gates generate alternating currents $I_1(t)$ and $I_2(t)$ at the leads. 230

9.5 The current cross-correlator \mathcal{P}_{12} , Eq. (9.73), as a function of the amplitude $U_{L,1}$ of a potential $U_L(t) = U_{L,0} + U_{L,1} \cos(\Omega_0 t + \varphi_L)$ acting upon the left capacitor, see Fig. 9.4. The three lines shown differ in the way that the right capacitor is driven: The right capacitor can be stationary (upper solid black line); driven by the potential $U_R(t) = U_{R,0} + U_{R,1} \cos(\Omega_0 t + \varphi_R)$, which is out of phase, $\varphi_R = \pi$, and has an amplitude $eU_{R,1} = 0.5\Delta_R$ (lower solid green line); or driven by the in-phase potential, $\varphi_R = 0$, with amplitude $eU_{R,1} = 0.5\Delta_R$ (dashed red line). Other parameters are $eU_{L,0} = eU_{R,0} = 0.25\Delta_R$ ($\Delta_L = \Delta_R$), $\varphi_L = 0$, and $T_L = T_R = 0.1$ 233

9.6 The mesoscopic electron collider with noisy single-particle sources. The two noisy flows originating from the quantum point contacts L and R can collide at the quantum point contact C . 238

9.7 The current cross-correlator \mathcal{P}_{12} as a function of the amplitude $U_{L,1}$ of a potential $U_L(t) = U_{L,0} + U_{L,1} \cos(\Omega_0 t + \varphi_L)$ driving the single-particle source S_L , see Fig. 9.6. The parameters of the single-particle sources S_L and S_R are the same as in Fig. 9.5 but $\varphi_L = \varphi_R$. Other parameters are $T_L = T_R = 0.5$ 239

9.8 A quantum electronic circuit comprising two single-particle sources S_L and S_R and two Mach–Zehnder interferometers with magnetic fluxes Φ_L and Φ_R 244

Chapter 1

Landauer–Büttiker formalism

According to the Landauer–Büttiker approach [1–6] the transport phenomena in mesoscopic [7, 8] conducting systems can be described with the help of a corresponding quantum-mechanical scattering problem. The mesoscopic system is assumed to be connected to macroscopic contacts acting as reservoirs of electrons, which are scattered by the mesoscopic sample. After scattering the electrons return to the original contact or go to a different one. Thus the problem of calculating such transport characteristics as, for example, electrical conductance or thermal conductance is reduced to solving a quantum-mechanical scattering problem with a potential profile corresponding to the sample under consideration [9] with possibly subsequent statistical averaging [10]. All information concerning transport properties of a sample is encoded in its scattering matrix, \hat{S} .

We concentrate on a single-particle scattering matrix. Therefore, we neglect electron-electron interactions and use the Schrödinger equation for spinless electrons as the basic equation. In principle interactions can be easily incorporated on the mean-field level.

1.1 Scattering matrix

In quantum mechanics an electron is characterized by the wave function, $\Psi(t, \mathbf{r})$, dependent on time t and on a spatial coordinate \mathbf{r} . If the wave function, $\Psi^{(in)}$, for an electron incident to the scatterer is known then using the Schrödinger equation one can calculate the wave function, $\Psi^{(out)}$, for a scattered electron. One can ask whether one needs to solve the Schrödinger equation for each $\Psi_j^{(in)}$? The answer is no. It is enough to solve the scattering problems for incident states $\psi_\alpha^{(in)}$ constituting the full orthonormal

basis. After that, using the superposition principle, one can find the solution for the scattering problem with arbitrary incident state, $\Psi_j^{(in)}$.

To this end we expand an incident electron wave function, $\Psi^{(in)}$, in the basis functions $\psi_\alpha^{(in)}$,

$$\Psi^{(in)} = \sum_{\alpha} a_{\alpha} \psi_{\alpha}^{(in)}. \quad (1.1)$$

Then we expand a wave function for the scattered electron, $\Psi^{(out)}$, in the basis functions $\psi_\alpha^{(out)}$,

$$\Psi^{(out)} = \sum_{\beta} b_{\beta} \psi_{\beta}^{(out)}. \quad (1.2)$$

The set of functions $\psi_\alpha^{(in)}$ and $\psi_\beta^{(out)}$ constitutes the full orthonormal basis.

The problem is to find the coefficients b_β if the set of coefficients a_α is known. First we consider an auxiliary problem, namely the scattering of an electron with wave function $\Psi_1^{(in)} = \psi_1^{(in)}$. In this case the set of coefficients in Eq. (1.1) is the following: $(1, 0, 0, \dots)$. The solution for this scattering problem we write as Eq. (1.2) with coefficients $S_{\beta 1}$,

$$\Psi_1^{(out)} = \sum_{\beta} S_{\beta 1} \psi_{\beta}^{(out)}. \quad (1.3)$$

The coefficient $S_{\beta 1}$ is a quantum-mechanical transition amplitude from the state $\psi_1^{(in)}$ to the state $\psi_\beta^{(out)}$. Note if the incident wave function is multiplied by some constant factor A then the wave function for a scattered state is also multiplied by the same factor,

$$\Psi_1^{(in)} = A \psi_1^{(in)} \quad \Rightarrow \quad \Psi_1^{(out)} = A \sum_{\beta} S_{\beta 1} \psi_{\beta}^{(out)}. \quad (1.4)$$

After solving the scattering problem with incident state $\Psi_\gamma^{(in)} = \psi_\gamma^{(in)}$ we find the coefficients $S_{\beta\gamma}$,

$$\Psi_\gamma^{(out)} = \sum_{\beta} S_{\beta\gamma} \psi_{\beta}^{(out)}. \quad (1.5)$$

With coefficients $S_{\alpha\beta}$ we can solve the scattering problem for an arbitrary incident state. Formally the corresponding algorithm is the following:

1. The wave function for an incident state is expanded into the series in basis functions $\psi_\alpha^{(in)}$, Eq. (1.1).

2. The scattered state wave function, $\Psi^{(out)}$, is represented as the sum of partial contributions, $\Psi_\alpha^{(out)}$, due to scattering of partial incident waves, $\Psi_\alpha^{(in)} = a_\alpha \psi_\alpha^{(in)}$,

$$\Psi^{(out)} = \sum_\alpha \Psi_\alpha^{(out)}, \quad (1.6)$$

$$\Psi_\alpha^{(out)} = a_\alpha \sum_\beta S_{\beta\alpha} \psi_\beta^{(out)}.$$

3. The coefficients b_β for the scattered state of interest, $\Psi^{(out)} = \sum_\alpha a_\alpha \sum_\beta S_{\beta\alpha} \psi_\beta^{(out)} \equiv \sum_\beta b_\beta \psi_\beta^{(out)}$, are the following

$$b_\beta = \sum_\alpha S_{\beta\alpha} a_\alpha. \quad (1.7)$$

Equation (1.7) solves the problem: It expresses the coefficients b_β for the scattered wave function in terms of the coefficients a_α for the incident wave function. It is convenient to treat the quantities, $S_{\beta\alpha}$, of Eq. (1.7) as the elements of some matrix, \hat{S} , which is referred to as *the scattering matrix*.¹

If the coefficients a_α and b_β are collected into vector columns

$$\hat{b} = \begin{pmatrix} b_1 \\ b_2 \\ \vdots \end{pmatrix}, \quad \hat{a} = \begin{pmatrix} a_1 \\ a_2 \\ \vdots \end{pmatrix}, \quad (1.8)$$

then the corresponding relations simplify to

$$\hat{b} = \hat{S}\hat{a}. \quad (1.9)$$

As we already mentioned, the scattering matrix elements, $S_{\alpha\beta}$, are quantum-mechanical amplitudes for a particle in the state $\psi_\beta^{(in)}$ to be scattered into the state $\psi_\alpha^{(out)}$. The order of indices is important. We use the convention that the first index (for the element $S_{\alpha\beta}$ it is α) corresponds to a scattered state while the second index corresponds to an incident state.

¹The scattering matrix elements are directly related to the corresponding single-particle Green's functions [11, 12]. For the generalization to the periodically driven case see Ref. [13].

1.1.1 Scattering matrix properties

General physical principles put some constraints on the scattering matrix elements.

1.1.1.1 Unitarity

Particle number conservation during scattering requires the scattering matrix to be unitary,

$$\hat{S}^\dagger \hat{S} = \hat{S} \hat{S}^\dagger = \hat{I}. \quad (1.10)$$

Here \hat{I} is a unit matrix of the same dimensions as \hat{S} ,

$$\hat{I} = \begin{pmatrix} 1 & 0 & 0 & \dots \\ 0 & 1 & 0 & \dots \\ 0 & 0 & 1 & \dots \\ & & & \dots \end{pmatrix}. \quad (1.11)$$

The elements of the matrix \hat{S}^\dagger are related to the elements of the scattering matrix \hat{S} in the following way: $(\hat{S}^\dagger)_{\alpha\beta} = (\hat{S})_{\beta\alpha}^*$. Therefore, the expanded equation (1.10) reads

$$\sum_{\alpha=1}^{N_r} S_{\alpha\beta}^* S_{\alpha\gamma} = \delta_{\beta\gamma}, \quad (1.12)$$

$$\sum_{\beta=1}^{N_r} S_{\alpha\beta} S_{\delta\beta}^* = \delta_{\alpha\delta}. \quad (1.13)$$

To prove unitarity, for instance, in the case when the wave function is normalized, i.e., it corresponds to scattering of a single particle, we use the integral over space for both the incident wave function and the scattered wave function:

$$\int d^3r |\Psi^{(in)}|^2 = \int d^3r |\Psi^{(out)}|^2 = 1. \quad (1.14)$$

Then we use Eqs. (1.1) and (1.2). For instance, for $\Psi^{(in)}$ we get,

$$\begin{aligned}
\int d^3r |\Psi^{(in)}|^2 &= \int d^3r \sum_{\alpha} a_{\alpha} \psi_{\alpha}^{(in)} \left(\sum_{\beta} a_{\beta}^* \psi_{\beta}^{(in)} \right)^* \\
&= \sum_{\alpha} \sum_{\beta} a_{\alpha} a_{\beta}^* \int d^3r \psi_{\alpha}^{(in)} \left(\psi_{\beta}^{(in)} \right)^* = \sum_{\alpha} \sum_{\beta} a_{\alpha} a_{\beta}^* \delta_{\alpha\beta} \\
&= \sum_{\alpha} |a_{\alpha}|^2 = 1.
\end{aligned} \tag{1.15}$$

Here we took into account that the functions $\psi_{\alpha}^{(in)}$ are orthonormal,

$$\int d^3r \psi_{\alpha}^{(in)} \left(\psi_{\beta}^{(in)} \right)^* = \delta_{\alpha\beta}, \tag{1.16}$$

where $\delta_{\alpha\beta}$ is the Kronecker symbol,

$$\delta_{\alpha\beta} = \begin{cases} 1, & \alpha = \beta, \\ 0, & \alpha \neq \beta. \end{cases} \tag{1.17}$$

By analogy we find for $\Psi^{(out)}$:

$$\sum_{\alpha} |b_{\alpha}|^2 = 1. \tag{1.18}$$

Therefore, from Eqs. (1.15) and (1.18) it follows that

$$\sum_{\alpha} |a_{\alpha}|^2 = \sum_{\alpha} |b_{\alpha}|^2. \tag{1.19}$$

Representing the coefficients a_{α} and b_{α} as vector columns, \hat{a} and \hat{b} , we write

$$\begin{aligned}
\sum_{\alpha} |a_{\alpha}|^2 &= \hat{a}^{\dagger} \hat{a}, \\
\sum_{\alpha} |b_{\alpha}|^2 &= \hat{b}^{\dagger} \hat{b}.
\end{aligned} \tag{1.20}$$

Next we take into account that $\hat{b} = \hat{S} \hat{a}$ and, correspondingly, $\hat{b}^{\dagger} = \hat{a}^{\dagger} \hat{S}^{\dagger}$ and finally calculate,

$$\hat{b}^\dagger \hat{b} = \hat{a}^\dagger \hat{S}^\dagger \hat{S} \hat{a} = \hat{a}^\dagger \hat{a}. \quad (1.21)$$

From the last equality the required relation, Eq. (1.10), follows directly.

Note, however, that for the particles with continuous spectrum, which we will consider, the wave function is normalized to the Dirac delta function rather than to unity. In such a case the scattering of particles with fixed incoming flow is a more natural problem. For instance, a plane wave e^{ikx} corresponds to a flow of particles with intensity $v = \hbar k/m$ rather than to a single particle. Charge conservation in this case (under stationary conditions) implies current conservation. Therefore, it is convenient to choose the basis functions normalized to carry a unit flux, see, e.g., Refs [5, 11]. Then we can say more precisely:

Equation (1.9) defines the scattering matrix \hat{S} if the vectors \hat{b} and \hat{a} are calculated using the unit flux basis.

The square of the modulus of a scattering matrix element defines an intensity of a scattered flow if the intensity of an incident flow is unity. Then the unitarity of the scattering matrix reflects particle flow conservation.

1.1.1.2 *Micro-reversibility*

Micro-reversibility is an invariant of the equations of motion under time reversal. Neither classical physics nor quantum physics makes a distinction between forward time and backward time.

If we change simultaneously, $t \rightarrow -t$ and $\mathbf{v} \rightarrow -\mathbf{v}$, then the classical equations of motion predict that the particle will move along the same trajectory but in the opposite direction. From the scattering theory point of view movement in the opposite direction means that the scattered particle becomes an incoming one and the incoming particle becomes a scattered one.

Quantum-mechanical formalism deals with states rather than with particles. The additional complication comes from the fact that the wave function is complex. To analyze micro-reversibility in quantum mechanics [14] we consider the Schrödinger equation

$$i\hbar \frac{\partial \Psi}{\partial t} = \mathcal{H} \Psi, \quad (1.22)$$

where \mathcal{H} is the Hamiltonian dependent on the momentum \mathbf{p} of a particle. Velocity reversal within classical physics is equivalent to a momentum

reversal within quantum physics. The Hamiltonian [and, correspondingly, Eq. (1.22)] is invariant under momentum reversal, $\mathcal{H}(\mathbf{p}) = \mathcal{H}(-\mathbf{p})$. While under time reversal the sign on the left hand side (LHS) of Eq. (1.22) is changed. On the other hand if simultaneously we use the complex conjugate equation and take into account that the Hamiltonian is Hermitian, $\mathcal{H}^* = \mathcal{H}$, then we find that the transformed equation for the complex conjugate wave function $\Psi^*(-t)$ is identical to the original equation for $\Psi(t)$,

$$i\hbar \frac{\partial(\Psi^*)}{\partial(-t)} = \mathcal{H}(\Psi^*). \quad (1.23)$$

We conclude: If the evolution in forward time is described by the wave function $\Psi(t)$ then the evolution in backward time is described by the complex conjugate function $\Psi^*(-t)$. For scattering theory this means that if initially the incident particle is in the state $\Psi^{(in)}(t)$ and the scattered particle is in the state $\Psi^{(out)}(t)$ then under time reversal the state $(\Psi^{(out)}(-t))^*$ is for an incident particle and the state $(\Psi^{(in)}(-t))^*$ is for a scattered particle.

Such symmetry results in various properties of the scattering matrix. To clarify these we will consider scattering in both forward and backward times in detail. The initial scattering process: $\Psi^{(in)}(t) = \sum_{\alpha} a_{\alpha} \psi_{\alpha}^{(in)}(t)$ is an incident wave and $\Psi^{(out)}(t) = \sum_{\beta} b_{\beta} \psi_{\beta}^{(out)}(t)$ is a scattered wave. The coefficients a_{α} and b_{β} are related through equation (1.9). The scattering process after time reversal: $(\Psi^{(out)}(-t))^* = \sum_{\beta} b_{\beta}^* (\psi_{\beta}^{(out)}(-t))^*$ is an incident wave and $(\Psi^{(in)}(-t))^* = \sum_{\alpha} a_{\alpha}^* (\psi_{\alpha}^{(in)}(-t))^*$ is a scattered wave. Under both time reversal and complex conjugation the basis functions for incident and scatterer states replace each other, $(\psi_{\beta}^{(out)}(-t))^* = \psi_{\beta}^{(in)}(t)$. Therefore, we can write

$$\begin{aligned} (\Psi^{(out)}(-t))^* &= \left(\sum_{\beta} b_{\beta} \psi_{\beta}^{(out)}(-t) \right)^* = \sum_{\beta} b_{\beta}^* \psi_{\beta}^{(in)}(t), \\ (\Psi^{(in)}(-t))^* &= \left(\sum_{\alpha} a_{\alpha} \psi_{\alpha}^{(in)}(-t) \right)^* = \sum_{\alpha} a_{\alpha}^* \psi_{\alpha}^{(out)}(t). \end{aligned} \quad (1.24)$$

Since the Hamiltonian and the basis functions remain invariant the scattering matrix is invariant as well. Therefore, the coefficients a_{α}^* and b_{β}^* in

Eq. (1.24) are related in the same way as the corresponding coefficients (b_β and a_α) in Eqs. (1.1) and (1.2),

$$\hat{a}^* = \hat{S} \hat{b}^*. \quad (1.25)$$

Thus the sets of coefficients \hat{a} and \hat{b} have to fulfill two equations, (1.9) and (1.25). From Eq. (1.9) we find,

$$\hat{a} = \hat{S}^{-1} \hat{b}, \quad (1.26)$$

where \hat{S}^{-1} is an inverse matrix, $\hat{S} \hat{S}^{-1} = \hat{S}^{-1} \hat{S} = \hat{I}$. Comparing Eqs. (1.26) and (1.25) we conclude that $\hat{S}^* = \hat{S}^{-1}$. Further, from the unitarity, Eq. (1.10), it follows that

$$\left. \begin{array}{l} \hat{S}^\dagger \hat{S} = \hat{I} \\ \hat{S}^{-1} \hat{S} = \hat{I} \end{array} \right\} \Rightarrow \hat{S}^\dagger = \hat{S}^{-1}. \quad (1.27)$$

Finally we conclude that micro-reversibility requires the scattering matrix to be invariant under the transposition operation. In other words, the scattering matrix elements are symmetric in their indices,

$$\hat{S} = \hat{S}^T \Rightarrow S_{\alpha\beta} = S_{\beta\alpha}. \quad (1.28)$$

Note the presence of a magnetic field H slightly changes the micro-reversibility condition: In addition to a time and a momentum reversal we need to invert the magnetic field direction, $H \rightarrow -H$. It is clear, for instance, from the Hamiltonian of a free particle with mass m and charge e propagating along the axis x in the presence of a magnetic field,

$$\mathcal{H} = \frac{(p_x - eA_x)^2}{2m},$$

where A_x is a vector potential projection onto the axis x . Note that $H = \text{rot } \mathbf{A}$. Thus in the presence of a magnetic field Eq. (1.28) is transformed [5]

$$\hat{S}(H) = \hat{S}^T(-H) \Rightarrow S_{\alpha\beta}(H) = S_{\beta\alpha}(-H). \quad (1.29)$$

In particular, the reflection amplitude, $\alpha = \beta$, is an even function for a magnetic field.

1.2 Current operator

Now we consider how the scattering matrix formalism can be applied to transport phenomena in mesoscopic samples. The scattering matrix relies on *the single-electron approximation*. Within this approximation the separate electrons are considered as independent particles whose interaction with other electrons, nuclei, impurities, quasi-particles, etc. can be described via the effective potential energy, $U_{eff}(t, \mathbf{r})$. Such an approach allows a simple and physically transparent description of transport phenomena on a qualitative level and in many cases even on a quantitative level.

Let us consider a mesoscopic sample connected to several, N_r , macroscopic contacts acting as electron reservoirs, Fig. 1.1. Electrons, propagating from some reservoir to the sample, enter it, are scattered inside it, and then leave it to go to the same or a different reservoir. To calculate the current flowing between the sample and the reservoirs we do not need to know what happens with each electron inside the sample. It is enough to look at the incoming and outgoing electron flows. To this end we enclose a sample by a fictitious surface Σ , see Fig. 1.1, and consider electron flows crossing this surface in the directions to the sample or back. In this case we, in fact, deal with the scattering problem: Electrons propagating to the sample are incident, or incoming, particles [we denote them via an upper index (*in*)], while electrons propagating from the sample are scattered, or outgoing, particles [upper index (*out*)]. We emphasize that we consider only elastic, i.e., energy-conserving, scattering. To neglect inelastic scattering we assume low temperatures when the phase coherence length, L_φ , is much larger than the size of a sample, $L_\varphi(T) \gg L$.

It is convenient to choose the eigen wave functions for electrons in leads connecting a scatterer to the reservoirs as the basis functions for defining the scattering matrix elements. These wave functions can be represented as the product of longitudinal and transverse terms. For the sake of simplicity we assume that the leads have only one conducting sub-band. Therefore, there is only one type of transverse wave function in each lead. We choose plane waves propagating to the scatterer (wave number $-k$) or from the scatterer (wave number k) as longitudinal wave functions. The former (latter) wave functions comprise the basis for incident, $\psi_\alpha^{(in)}$, (scattered, $\psi_\alpha^{(out)}$) electrons.

To calculate the current flowing between the scatterer and the reservoirs we use the second quantization formalism. This formalism deals with

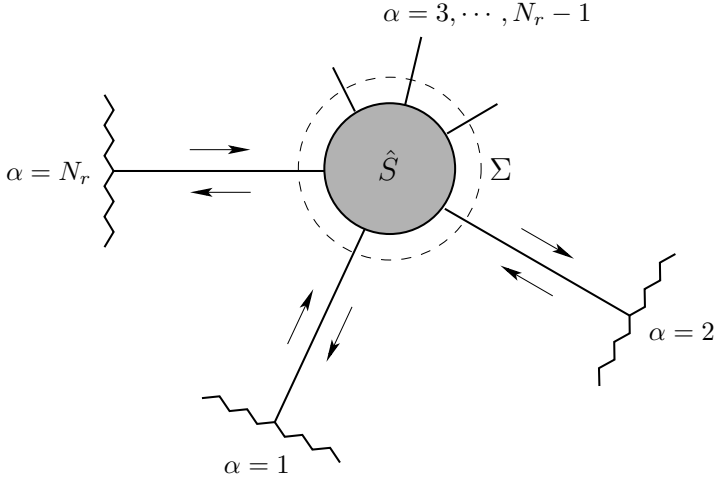


Fig. 1.1 A mesoscopic sample with scattering matrix \hat{S} . The index $\alpha = 1, 2, \dots, N_r$ numbers electron reservoirs. The arrows directed to (from) the scatterer show a propagation direction for incident (scattered) electrons. The electron flow is calculated at the surface Σ shown as a dashed line.

operators creating/annihilating particles in some quantum state. We use different operators corresponding to incident electrons, $\hat{a}_\alpha^\dagger(E)/\hat{a}_\alpha(E)$, and to scattered electrons, $\hat{b}_\alpha^\dagger(E)/\hat{b}_\alpha(E)$. The operator $\hat{a}_\alpha^\dagger(E)$ creates one electron in the state with wave function $\psi_\alpha^{(in)}(E)/\sqrt{\hbar v_\alpha(E)}$, while the operator $\hat{b}_\alpha^\dagger(E)$ creates one electron in the state with wave function $\psi_\alpha^{(out)}(E)/\sqrt{\hbar v_\alpha(E)}$. The factor $1/\sqrt{\hbar v_\alpha(E)}$ takes account of the unit flux normalization. Note the index α can be composite, i.e., it can include, apart from the reservoir's number, the additional sub-indices, for instance, a sub-band number, an electron spin, etc.

Introduced fermionic operators are subject to the following anti-commutation relations:

$$\begin{aligned} \hat{a}_\alpha^\dagger(E) \hat{a}_\beta(E') + \hat{a}_\beta(E') \hat{a}_\alpha^\dagger(E) &= \delta_{\alpha\beta} \delta(E - E'), \\ \hat{b}_\alpha^\dagger(E) \hat{b}_\beta(E') + \hat{b}_\beta(E') \hat{b}_\alpha^\dagger(E) &= \delta_{\alpha\beta} \delta(E - E'). \end{aligned} \tag{1.30}$$

Next we introduce the field operators for electrons in lead α ,

$$\hat{\Psi}_\alpha(t, \mathbf{r}) = \frac{1}{\sqrt{2\pi}} \int_0^\infty dE e^{-i\frac{E}{\hbar}t} \left\{ \hat{a}_\alpha(E) \frac{\psi_\alpha^{(in)}(E, \mathbf{r})}{\sqrt{\hbar v_\alpha(E)}} + \hat{b}_\alpha(E) \frac{\psi_\alpha^{(out)}(E, \mathbf{r})}{\sqrt{\hbar v_\alpha(E)}} \right\}, \quad (1.31)$$

$$\hat{\Psi}_\alpha^\dagger(t, \mathbf{r}) = \frac{1}{\sqrt{2\pi}} \int_0^\infty dE e^{i\frac{E}{\hbar}t} \left\{ \hat{a}_\alpha^\dagger(E) \frac{\psi_\alpha^{(in)*}(E, \mathbf{r})}{\sqrt{\hbar v_\alpha(E)}} + \hat{b}_\alpha^\dagger(E) \frac{\psi_\alpha^{(out)*}(E, \mathbf{r})}{\sqrt{\hbar v_\alpha(E)}} \right\}.$$

Here $v_\alpha(E) = \hbar k_\alpha(E)/m$ is an electron's velocity, $\mathbf{r} = (x, r_\perp)$, with x longitudinal and r_\perp transverse spatial coordinates within the lead α . Note that $1/(\hbar v_\alpha(E))$ is the density of states, $(2\pi)^{-1} dk/dE$, for a one-dimensional conductor.

Using the field operators we write the operator, \hat{I}_α , for a current flowing in the lead α

$$\hat{I}_\alpha(t, x) = \frac{i\hbar e}{2m} \int dr_\perp \left\{ \frac{\partial \hat{\Psi}_\alpha^\dagger(t, \mathbf{r})}{\partial x} \hat{\Psi}_\alpha(t, \mathbf{r}) - \hat{\Psi}_\alpha^\dagger(t, \mathbf{r}) \frac{\partial \hat{\Psi}_\alpha(t, \mathbf{r})}{\partial x} \right\}. \quad (1.32)$$

Here the positive direction is from the scatterer to the reservoir.

Next we represent the basis wave functions as the product of transverse and longitudinal parts,

$$\begin{aligned} \psi^{(in)}(E, \mathbf{r}) &= \xi_E(r_\perp) e^{-ik(E)x}, \\ \psi^{(out)}(E, \mathbf{r}) &= \xi_E(r_\perp) e^{ik(E)x}, \end{aligned} \quad (1.33)$$

and take into account that the transverse wave functions are normalized,

$$\int dr_\perp |\xi_E(r_\perp)|^2 = 1. \quad (1.34)$$

In what follows we are interested in currents flowing under the bias much smaller than the Fermi energy, μ_0 . Therefore, in all equations the main contribution comes from energies within the interval that are much smaller than the energy itself,²

²In the case of a stationary current this restriction can be safely relaxed since the calculation of an expectation value implies $E = E'$. While for calculation of a time-dependent current or a noise and higher current cumulants (even in the stationary case) the restriction (1.35) is important.

$$|E - E'| \ll E \sim \mu_0. \quad (1.35)$$

The last inequality allows us to strongly simplify the equation for a current. We can put, $v(E) \approx v(E')$ and $k(E) \approx k(E')$. Moreover, within the same sub-band the transverse wave functions are the same, $\xi_E = \xi_{E'}$. Note if the functions ξ_E and $\xi_{E'}$ are from different sub-bands then they are orthogonal, $\int dr_\perp \xi_E(r_\perp) \left(\xi_{E'}(r_\perp) \right)^* = 0$. That allows us to split the total current into the sum of contributions from different sub-bands. Therefore, we can assume each lead having only one sub-band.

Substituting Eq. (1.31) into Eq. (1.32) and taking into account Eq. (1.35) we calculate

$$\begin{aligned} \hat{I}_\alpha(t, x) &= \frac{i\hbar e}{2m} \iint dE dE' e^{i\frac{E-E'}{\hbar}t} \int dr_\perp |\xi_{E,\alpha}(r_\perp)|^2 \\ &\times \left\{ \frac{\partial}{\partial x} \left[\hat{a}_\alpha^\dagger(E) e^{ik_\alpha(E)x} + \hat{b}_\alpha^\dagger(E) e^{-ik_\alpha(E)x} \right] \left(\hat{a}_\alpha(E') e^{-ik_\alpha(E')x} + \hat{b}_\alpha(E') e^{ik_\alpha(E')x} \right) \right. \\ &\left. - \left(\hat{a}_\alpha^\dagger(E) e^{ik_\alpha(E)x} + \hat{b}_\alpha^\dagger(E) e^{-ik_\alpha(E)x} \right) \frac{\partial}{\partial x} \left[\hat{a}_\alpha(E') e^{-ik_\alpha(E')x} + \hat{b}_\alpha(E') e^{ik_\alpha(E')x} \right] \right\}. \end{aligned}$$

Differentiating over x and combining similar terms we finally arrive at the following equation for the current operator [5],

$$\hat{I}_\alpha(t) = \frac{e}{\hbar} \iint dE dE' e^{i\frac{E-E'}{\hbar}t} \left\{ \hat{b}_\alpha^\dagger(E) \hat{b}_\alpha(E') - \hat{a}_\alpha^\dagger(E) \hat{a}_\alpha(E') \right\}. \quad (1.36)$$

In what follows we use this equation and calculate, in particular, a measurable current, $I_\alpha = \langle \hat{I}_\alpha \rangle$, flowing into the lead α . Here $\langle \dots \rangle$ stands for quantum-statistical averaging over the state of incoming electrons. To calculate such an average for the products of $\hat{a}^\dagger \hat{a}$ and $\hat{b}^\dagger \hat{b}$ we take into account that the creation and annihilation operators, \hat{a}_α^\dagger and \hat{a}_α , correspond to particles propagating from the reservoir. We suppose that the presence of a mesoscopic scatterer does not affect the equilibrium properties of reservoirs. Therefore, the incoming particles are equilibrium particles of macroscopic reservoirs. And for them we can use the standard rules for calculating the quantum-statistical average of the product of creation and annihilation operators. In addition we suppose that electrons at different reservoirs, $\alpha \neq \beta$, are not correlated. Then we can write

$$\begin{aligned}\langle \hat{a}_\alpha^\dagger(E) \hat{a}_\beta(E') \rangle &= \delta_{\alpha\beta} \delta(E - E') f_\alpha(E), \\ \langle \hat{a}_\alpha(E) \hat{a}_\beta^\dagger(E') \rangle &= \delta_{\alpha\beta} \delta(E - E') \{1 - f_\alpha(E)\},\end{aligned}\tag{1.37}$$

where $f_\alpha(E)$ is the Fermi distribution function [15] for electrons in the reservoir α ,

$$f_\alpha(E) = \frac{1}{1 + e^{\frac{E - \mu_\alpha}{k_B T_\alpha}}}.\tag{1.38}$$

Here k_B is the Boltzmann constant, μ_α is the Fermi energy (the electrochemical potential) and T_α is the temperature of the reservoir α .

In contrast the operators \hat{b}_α^\dagger and \hat{b}_α correspond to scattered particles which, in general, are non-equilibrium particles. To calculate the quantum-statistical average for (the product of) them we need to express them in terms of the operators for incoming particles for which we know how to calculate a corresponding average. To this end we consider both the field operator, $\hat{\Psi}^{(in)}$, corresponding to an incoming wave,

$$\hat{\Psi}^{(in)} = \sum_{\alpha=1}^{N_r} \hat{a}_\alpha \frac{\psi_\alpha^{(in)}}{\sqrt{\hbar v_\alpha}},$$

and the field operator, $\hat{\Psi}^{(out)}$, corresponding to a scattered wave,

$$\hat{\Psi}^{(out)} = \sum_{\beta=1}^{N_r} \hat{b}_\beta \frac{\psi_\beta^{(out)}}{\sqrt{\hbar v_\beta}}.$$

These equations are similar to Eqs. (1.1) and (1.2) excepting the coefficients are now the second quantization operators. Thus each of the operators \hat{b}_β is expressed in terms of all the operators \hat{a}_α through the elements of the scattering matrix, which is an $N_r \times N_r$ unitary matrix. By analogy with Eq. (1.7) we write [5]

$$\begin{aligned}\hat{b}_\alpha &= \sum_{\beta=1}^{N_r} S_{\alpha\beta} \hat{a}_\beta, \\ \hat{b}_\alpha^\dagger &= \sum_{\beta=1}^{N_r} S_{\alpha\beta}^* \hat{a}_\beta^\dagger.\end{aligned}\tag{1.39}$$

The equations (1.36)–(1.39) constitute the basis of the scattering matrix approach to transport phenomena in mesoscopic physics.

1.3 Direct current and the distribution function

Let us calculate a current, I_α ,

$$I_\alpha = \langle \hat{I}_\alpha \rangle, \quad (1.40)$$

flowing into the lead α under the DC bias, $\Delta V_{\alpha\beta} = V_\alpha - V_\beta$. In this case the different reservoirs have different electrochemical potentials,

$$\mu_\alpha = \mu_0 + eV_\alpha. \quad (1.41)$$

Note we include the potential energy eV_α in the μ_α . Then the energy E means the total (kinetic plus potential) energy of an electron. The use of a total energy (instead of a kinetic one) is convenient since it is conserved (in the stationary case) while an electron propagates from one reservoir through the scatterer to another reservoir.

The current operator, $\hat{I}_\alpha(t)$, is given in Eq. (1.36). After averaging Eq. (1.40) reads

$$I_\alpha = \frac{e}{h} \int dE \left\{ f_\alpha^{(out)}(E) - f_\alpha^{(in)}(E) \right\}, \quad (1.42)$$

where we have introduced the distribution functions for incident electrons, $f_\alpha^{(in)}$, and for scattered electrons, $f_\alpha^{(out)}$,

$$\begin{aligned} \langle \hat{a}_\alpha^\dagger(E) \hat{a}_\alpha(E') \rangle &= \delta(E - E') f_\alpha^{(in)}(E), \\ \langle \hat{b}_\alpha^\dagger(E) \hat{b}_\alpha(E') \rangle &= \delta(E - E') f_\alpha^{(out)}(E). \end{aligned} \quad (1.43)$$

The physical meaning for the introduced distribution functions is that the quantity $\frac{dE}{h} f_\alpha^{(in/out)}(E)$ defines the average number of electrons with an energy within the interval dE near E crossing the cross-section of the lead

α in unit time to/from the scatterer. The direct current is obviously the difference of the flows times an electron charge e .

According to Eq. (1.37) the distribution function for incoming electrons is the Fermi function for a corresponding reservoir,

$$f_{\alpha}^{(in)}(E) = f_{\alpha}(E). \quad (1.44)$$

To calculate the distribution function for scattered electrons, $f_{\alpha}^{(out)}(E)$, we use Eqs. (1.39), (1.37) and find,

$$\begin{aligned} \delta(E - E') f_{\alpha}^{(out)}(E) &\equiv \langle \hat{b}_{\alpha}^{\dagger}(E) \hat{b}_{\alpha}(E') \rangle \\ &= \sum_{\beta=1}^{N_r} \sum_{\gamma=1}^{N_r} S_{\alpha\beta}^*(E) S_{\alpha\gamma}^*(E') \langle \hat{a}_{\beta}^{\dagger}(E) \hat{a}_{\gamma}(E') \rangle \\ &= \sum_{\beta=1}^{N_r} \sum_{\gamma=1}^{N_r} S_{\alpha\beta}^*(E) S_{\alpha\gamma}^*(E') \delta(E - E') \delta_{\beta\gamma} f_{\beta}(E). \end{aligned}$$

Therefore, the distribution function, $f_{\alpha}^{(out)}(E)$, for electrons scattered into the lead α depends on the Fermi functions, $f_{\beta}(E)$, for all the reservoirs, $\beta = 1, 2, \dots, N_r$:

$$f_{\alpha}^{(out)}(E) = \sum_{\beta=1}^{N_r} |S_{\alpha\beta}(E)|^2 f_{\beta}(E). \quad (1.45)$$

Note if all the reservoirs have the same electrochemical potentials and temperatures (hence the same Fermi functions), $f_{\beta} = f_0, \forall \beta$, then the distribution function for scattered electrons is the Fermi function as well, i.e., the scattered electrons are in equilibrium. To show this we use the unitarity of the scattering matrix,

$$\hat{S}\hat{S}^{\dagger} = \hat{I} \quad \Rightarrow \quad \sum_{\beta=1}^{N_r} |S_{\alpha\beta}(E)|^2 = 1, \quad (1.46)$$

and find $f_{\alpha}^{(out)}(E) = f_0(E) \sum_{\beta=1}^{N_r} |S_{\alpha\beta}(E)|^2 = f_0(E)$. In contrast, if the potentials or temperatures of different reservoirs are different then the scattered electrons are characterized by the non-equilibrium distribution function, Fig. 1.2.

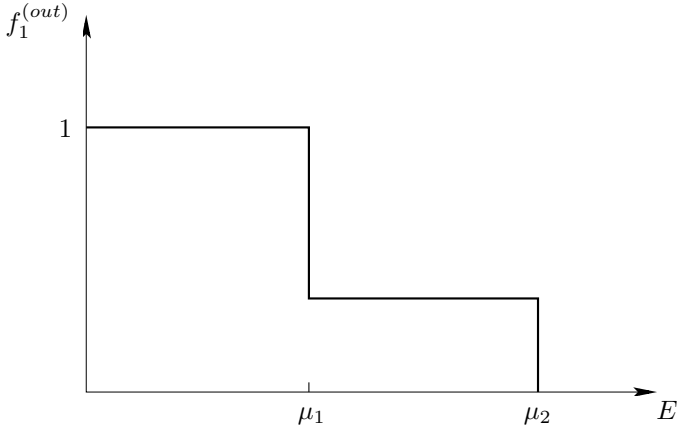


Fig. 1.2 The distribution function for electrons scattered into the contact $\alpha = 1$. The height of a step at $E = \mu_1$ is $|S_{12}|^2$. The scatterer is connected to two electron reservoirs at zero temperature, $T_1 = T_2 = 0$, and having chemical potentials μ_1 and μ_2 .

Substituting Eqs. (1.44) and (1.45) into Eq. (1.42) and using Eq. (1.46) we finally calculate a direct current,

$$I_\alpha = \frac{e}{h} \int dE \sum_{\beta=1}^{N_r} |S_{\alpha\beta}(E)|^2 \{f_\beta(E) - f_\alpha(E)\}. \quad (1.47)$$

We see that the current flowing into the lead α depends on the difference of the Fermi functions times the corresponding square of the scattering matrix element modulus. If all the reservoirs have the same potentials and temperatures then the current is zero. Otherwise there is a current through the sample.

1.3.1 Conservation of a direct current

Let us check whether Eq. (1.47) fulfills a direct current conservation law,

$$\sum_{\alpha=1}^{N_r} I_\alpha = 0, \quad (1.48)$$

which is a direct consequence of no charge accumulation inside the mesoscopic sample. This equation tells us that the sum of the current flowing into all the leads is zero. To avoid misunderstanding we stress that in each lead the positive direction is chosen from the scatterer to the corresponding

reservoir. Therefore, the current has a sign “+” or “-” if it is directed from or to the scatterer.

First of all we derive Eq. (1.48). To this end we use the electrical charge continuity equation,

$$\operatorname{div} \mathbf{j} + \frac{\partial \rho}{\partial t} = 0, \quad (1.49)$$

where \mathbf{j} is a current density vector and ρ is a charge density. We integrate it over the volume enclosed by the surface Σ (see Fig. 1.1). Then transforming the volume integral of a current density divergence into the surface integral of a current density and taking into account that the current flows into the leads only we arrive at the following

$$\sum_{\alpha=1}^{N_r} I_{\alpha}(t) + \frac{\partial Q}{\partial t} = 0. \quad (1.50)$$

Here Q is the charge on the scatterer. In the stationary case under consideration there are only direct currents in the leads and the charge Q is constant. Then Eq. (1.50) results in Eq. (1.48). In the non-stationary case we should average Eq. (1.50) over time. With the following definition of a direct current, $I_{\alpha} = \lim_{\mathcal{T} \rightarrow \infty} \frac{1}{\mathcal{T}} \int_0^{\mathcal{T}} dt I_{\alpha}(t)$, and assuming that the charge $Q(t)$ is bounded we again conclude that Eq. (1.48) is a consequence of Eq. (1.50).

Now we check whether Eq. (1.47) does satisfy Eq. (1.48). We use the unitarity of the scattering matrix in a form slightly different from but still equivalent to Eq. (1.46)

$$\hat{S}^{\dagger} \hat{S} = \hat{I} \quad \Rightarrow \quad \sum_{\alpha=1}^{N_r} |S_{\alpha\beta}(E)|^2 = 1. \quad (1.51)$$

Then from Eq. (1.47) we get

$$\begin{aligned} \sum_{\alpha=1}^{N_r} I_{\alpha} &= \frac{e}{h} \int dE \sum_{\alpha=1}^{N_r} \sum_{\beta=1}^{N_r} |S_{\alpha\beta}(E)|^2 \left\{ f_{\beta}(E) - f_{\alpha}(E) \right\} \\ &= \frac{e}{h} \int dE \left\{ \sum_{\beta=1}^{N_r} f_{\beta}(E) \sum_{\alpha=1}^{N_r} |S_{\alpha\beta}(E)|^2 - \sum_{\alpha=1}^{N_r} f_{\alpha}(E) \sum_{\beta=1}^{N_r} |S_{\alpha\beta}(E)|^2 \right\} \\ &= \frac{e}{h} \int dE \left\{ \sum_{\beta=1}^{N_r} f_{\beta}(E) - \sum_{\alpha=1}^{N_r} f_{\alpha}(E) \right\} = 0, \end{aligned}$$

as expected. Therefore, we have illustrated the earlier mentioned connection between unitarity and current conservation. Next we will use Eq. (1.47) and calculate a current in two simple but generic cases.

1.3.2 Difference of potentials

Let the reservoirs have different potentials but the same temperature

$$\begin{aligned}\mu_\alpha &= \mu_0 + eV_\alpha, \quad eV_\alpha \ll \mu_0, \\ T_\alpha &= T_0, \quad \forall \alpha.\end{aligned}\tag{1.52}$$

If $|eV_\alpha| \ll k_B T_0$ we can expand

$$f_\alpha = f_0 - eV_\alpha \frac{\partial f_0}{\partial E} + \mathcal{O}(V_\alpha^2),$$

where f_0 is the Fermi function with a chemical potential μ_0 and a temperature T_0 . Using this expansion in Eq. (1.47) we calculate a current

$$I_\alpha = \sum_{\beta=1}^{N_r} G_{\alpha\beta} \{V_\beta - V_\alpha\},\tag{1.53}$$

where we introduce the elements of the conductance matrix

$$G_{\alpha\beta} = G_0 \int dE \left(-\frac{\partial f_0}{\partial E} \right) |S_{\alpha\beta}(E)|^2,\tag{1.54}$$

with $G_0 = e^2/h$ the conductance quantum (for spinless electrons). Taking into account electron spin the conductance quantum should be doubled.

At zero temperature, $T_0 = 0$,

$$-\frac{\partial f_0}{\partial E} = \delta(E - \mu_0),$$

and the integration over energy in Eq. (1.54) becomes trivial. In this case the conductance matrix elements become especially simple [5]

$$G_{\alpha\beta} = G_0 \left| S_{\alpha\beta}(\mu_0) \right|^2. \quad (1.55)$$

It is clear that the linear dependence of a current on the potential difference is kept at a relatively small bias. The corresponding scale is dictated by the energy dependence of the scattering matrix elements, $S_{\alpha\beta}(E)$. To illustrate it we calculate a direct current at zero temperature, $T_0 = 0$, but finite potential, $eV_\alpha \neq 0$. In this case we cannot expand the Fermi function in powers of a potential, therefore, Eq. (1.47) becomes

$$I_\alpha = \frac{G_0}{e} \sum_{\beta=1}^{N_r} \int_{\mu_0+eV_\alpha}^{\mu_0+eV_\beta} dE |S_{\alpha\beta}(E)|^2. \quad (1.56)$$

If the quantity $G_{\alpha\beta}$ changes only a little within the energy interval $\sim |eV_\beta - eV_\alpha|$ near the Fermi energy μ_0 then we can use $S_{\alpha\beta}(E) \approx S_{\alpha\beta}(\mu_0)$ in Eq. (1.56), which results in linear I - V characteristics, Eq. (1.53).

On the other hand if one cannot ignore the energy dependence of $S_{\alpha\beta}(E)$ then the current becomes a non-linear function of a bias. As a simple example we consider a sample with two leads ($\alpha = 1, 2$) whose scattering properties are governed by the resonance level of a width Γ located at the energy E_1 :

$$|S_{12}(E)|^2 = \frac{\Gamma^2}{(E - E_1)^2 + \Gamma^2}. \quad (1.57)$$

For simplicity suppose that $E_1 = \mu_0$. Then substituting the equation above into Eq. (1.56) we find a current

$$I_1 = \frac{e}{h} \Gamma \left\{ \arctan\left(\frac{eV_2}{\Gamma}\right) - \arctan\left(\frac{eV_1}{\Gamma}\right) \right\}. \quad (1.58)$$

If the potentials are small compared to the resonance level width, $|eV_1|, |eV_2| \ll \Gamma$, we recover Ohm's law, $I_{12} = G_0 (V_1 - V_2)$. While in the opposite case, $|eV_1|, |eV_2| \gg \Gamma$, the current is an essentially non-linear function of potentials, $I_1 = (\Gamma^2/h) (V_1^{-1} - V_2^{-1})$. Therefore, we see that in this problem the level width Γ is a relevant energy scale.

1.3.3 Difference of temperatures

The temperature difference also can result in a current. This is the so-called *thermoelectric current*. To calculate it we suppose that the reservoirs have the same potentials but their temperatures are different,

$$\begin{aligned}\mu_\alpha &= \mu_0, \quad \forall \alpha, \\ T_\alpha &= T_0 + \mathcal{T}_\alpha, \quad \mathcal{T}_\alpha \ll T_0.\end{aligned}\tag{1.59}$$

Expanding the Fermi functions in Eq. (1.47) in powers of \mathcal{T}_α ,

$$f_\alpha = f_0 + \mathcal{T}_\alpha \frac{\partial f_0}{\partial T} + \mathcal{O}(\mathcal{T}_\alpha^2),$$

and taking into account that

$$\frac{\partial f_0}{\partial T} = -\frac{E - \mu_0}{T_0} \frac{\partial f_0}{\partial E},$$

we calculate the thermoelectric current flowing into the lead α ,

$$I_\alpha = \sum_{\beta=1}^{N_r} G_{\alpha\beta}^{(T)} \{ \mathcal{T}_\beta - \mathcal{T}_\alpha \}.\tag{1.60}$$

Here we have introduced the thermoelectric conductance matrix elements,

$$G_{\alpha\beta}^{(T)}(E) = \frac{\pi^2 e}{3h} k_B T_0 \frac{\partial |S_{\alpha\beta}(E)|^2}{\partial E},\tag{1.61}$$

and used the following integral

$$\int_0^\infty dE \frac{e^{\frac{E-\mu_0}{k_B T_0}}}{\left(1 + e^{\frac{E-\mu_0}{k_B T_0}}\right)^2} \left(\frac{E - \mu_0}{k_B T_0}\right)^2 = \frac{\pi^2}{3} k_B T_0.$$

From Eq. (1.61) it follows that if the conductance is energy independent, $G_{\alpha\beta}(E) = \text{const}$, then the thermoelectric conductance (and the thermoelectric current) is zero.

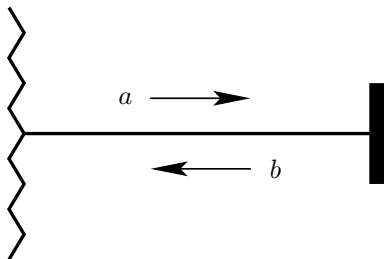


Fig. 1.3 A single-channel scatterer. a is the amplitude of an incoming wave, b is the amplitude of a reflected wave. A zigzag line denotes an electron reservoir.

1.4 Examples

Now we consider several examples to clarify the physical meaning of the scattering matrix elements. The scattering matrix is a square matrix $N_r \times N_r$, where N_r is the number of one-dimensional conducting sub-bands in each lead, connecting a mesoscopic sample to the reservoirs. N_r is the number of *scattering channels*.

1.4.1 Scattering matrix 1×1

Such a matrix has only one element, S_{11} , and it describes a sample connected to a single reservoir via a one-dimensional lead, Fig. 1.3. Sometimes such a sample is referred to as a *mesoscopic capacitor*.³ Unitarity, Eq. (1.10), requires $|S_{11}|^2 = 1$. Therefore, quite generally the scattering matrix 1×1 reads

$$\hat{S} = e^{i\gamma}, \quad (1.62)$$

where i is an imaginary unity, γ is real. Scattering in this case is reduced to the total reflection of an incident wave. Therefore, the element S_{11} is *the reflection coefficient*. Generally speaking any diagonal element, $S_{\alpha\alpha}$, of the scattering matrix of a higher dimension is a reflection coefficient, since it defines both the amplitude and the phase of a wave returning to the same reservoir where the incident wave originated. In the case under consideration (1×1) the amplitude of the wave remains the same, while

³More precisely it is one of the capacitor's plates.

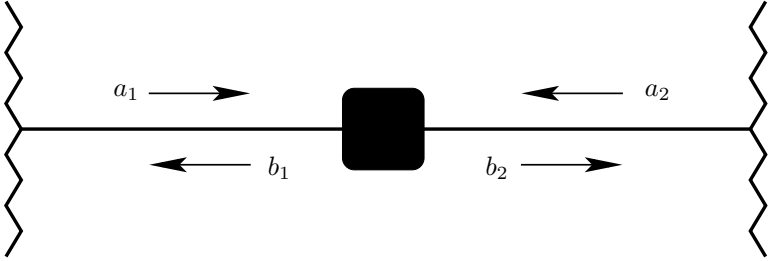


Fig. 1.4 A two-channel scatterer. a_α (b_α) are the amplitudes of incoming (scattered) waves, $\alpha = 1, 2$.

the phase is changed by γ , which is the only quantity encoding information about the properties of the mesoscopic sample. For instance, if the wave is reflected by a hard and infinite potential wall then the phase is changed by $\gamma = \pi$, while if the scatterer is a ring then γ depends on the magnetic flux threading the ring, and so on.

1.4.2 Scattering matrix 2×2

This matrix has in general four complex elements, hence there are eight real parameters. However, unitarity, Eq. (1.10), imposes four constraints. As a result there are only four independent parameters. It is convenient to choose the following independent parameters:

1. $R = |S_{11}|^2$ – a reflection probability.
2. γ – a phase relating to an effective charge, Q , of a scatterer via the Friedel sum rule, $Q = e/(2\pi i) \ln(\det \hat{S}) = e\gamma/\pi$ [16, 17].
3. θ – a phase characterizing the reflection asymmetry, $\theta = i \ln(S_{11}/S_{22})/2$.
4. ϕ – a phase characterizing the transmission asymmetry, $\phi = i \ln(S_{12}/S_{21})/2$. This phase depends on an external magnetic field or on an internal magnetic moment of a scatterer.

Therefore, the general expression for the scattering matrix 2×2 , describing a sample connected to two electron reservoirs, Fig. 1.4, can be written as follows

$$\hat{S} = e^{i\gamma} \begin{pmatrix} \sqrt{R} e^{-i\theta} & i\sqrt{1-R} e^{-i\phi} \\ i\sqrt{1-R} e^{i\phi} & \sqrt{R} e^{i\theta} \end{pmatrix}. \quad (1.63)$$

Note the reflection probability is the same in both scattering channels,

$$|S_{11}|^2 = |S_{22}|^2 = R. \quad (1.64)$$

The same is valid with respect to the transmission probabilities: they are independent of the direction of movement,

$$|S_{12}|^2 = |S_{21}|^2. \quad (1.65)$$

In addition the symmetry condition, Eq. (1.29), restricts the possible dependence of the parameters chosen for the magnetic field. It is easy to see that $\gamma(H)$, $R(H)$, and $\theta(H)$ are even functions, while $\phi(H)$ is an odd function, $\phi(H) = -\phi(-H)$. In particular, if $H = 0$ then $\phi = 0$ and, correspondingly, the transmission amplitude is independent of the movement direction,

$$S_{12}(H = 0) = S_{21}(H = 0). \quad (1.66)$$

We stress that Eq. (1.65) holds also in the presence of a magnetic field.

Turning to the transport properties, we see that the conductance, $G \equiv G_{12} = G_{21}$, of a sample with two leads is an even function of a magnetic field [5, 18]

$$G(H) = G(-H). \quad (1.67)$$

As we will show this property holds also for a sample with two quasi-one-dimensional leads. This symmetry is a consequence of the micro-reversibility of the quantum-mechanical equations of motion that are valid in the absence of inelastic interactions breaking the phase coherence.⁴

1.4.3 Scattering matrix 3×3

Such a matrix describes a scatterer connected to three reservoirs, Fig. 1.5. It has many, namely nine, independent real parameters, which makes it difficult to find a general expression. Usually the particular expressions for the

⁴In the non-linear regime and in the presence of electron-electron interactions the current through the two terminal sample is not an even function of a magnetic field [19, 20].

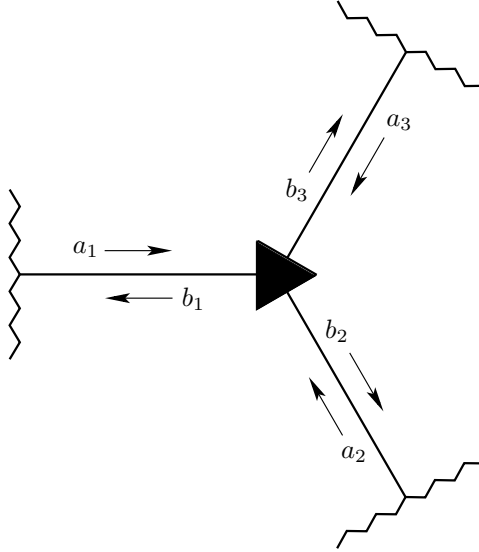


Fig. 1.5 A three-channel scatterer. a_α (b_α) are amplitudes of incoming (scattered) waves, $\alpha = 1, 2, 3$.

scattering matrix elements are used. For instance, following Refs. [21, 22] one can write a one-parametric scattering matrix

$$\hat{S} = \begin{pmatrix} -(a+b) & \sqrt{\epsilon} & \sqrt{\epsilon} \\ \sqrt{\epsilon} & a & b \\ \sqrt{\epsilon} & b & a \end{pmatrix}, \quad (1.68)$$

where $a = (\sqrt{1-2\epsilon} - 1)/2$, $b = (\sqrt{1-2\epsilon} + 1)/2$, and the real parameter ϵ changes within the following interval $0 \leq \epsilon \leq 0.5$. The parameter ϵ characterizes the coupling strength between the lead $\alpha = 1$ and the scatterer. At $\epsilon = 0$ this lead is decoupled completely from the scatterer, $S_{11} = -1$, while electrons freely propagate from the lead $\alpha = 2$ into the lead $\alpha = 3$ and back, $S_{32} = S_{23} = 1$. The limit $\epsilon = 0.5$ corresponds to a reflectionless coupling between the sample and the lead $\alpha = 1$: $S_{11} = 0$.

Sometimes, solving the Schrödinger equation for the junction of three one-dimensional leads, the Griffith boundary conditions are used [23]. These conditions include both the continuity of a wave function and a current conservation at a crossing point. Then a scattering matrix of the type given in Eq. (1.68) with parameter $\epsilon = 4/9$ arises. Other values of the

parameter ϵ , for instance, can be understood as related to the presence of some tunnel barrier at the crossing point.

It should be noted that in contrast to the two-lead case, see Eq. (1.64), in the case of three leads, the reflection probabilities $R_{\alpha\alpha} \equiv |S_{\alpha\alpha}|^2$, $\alpha = 1, 2, 3$, for different scattering channels can be different. Moreover, the current flowing between any two leads depends not only on the corresponding transmission probability, $T_{\alpha\beta} \equiv |S_{\alpha\beta}|^2$, $\alpha \neq \beta$, but also on the transmission probabilities to the third lead, $T_{\gamma\alpha}$ and $T_{\gamma\beta}$, $\gamma \neq \alpha, \beta$.

1.4.4 Scatterer with two leads

We will show that the conductance of a mesoscopic sample with two quasi-one-dimensional leads is an even function of a magnetic field. We saw this before, see Eq. (1.67), for the case of two one-dimensional leads when the scattering matrix is a 2×2 unitary matrix. Now we generalize this result onto the case when each lead has several conducting sub-bands [24].

Let one of the leads, say the left, have N_L conducting sub-bands while another one, the right, has N_R conducting sub-bands. The total number of scattering channels is $N_r = N_L + N_R$, therefore, the scattering matrix is an $N_r \times N_r$ unitary matrix. It is convenient to number the scattering channels in such a way that the first N_L scattering channels, $1 \leq \alpha \leq N_L$, correspond to the left lead, while the last N_R scattering channels, $N_L + 1 \leq \alpha \leq N_r$, correspond to the right lead. We assume that the left reservoir has a potential $-V/2$ while the right reservoir has a potential $V/2$. Note for all the sub-bands belonging to the same lead the corresponding potential V_α is the same,

$$V_\alpha = \begin{cases} -\frac{V}{2}, & 1 \leq \alpha \leq N_L, \\ \frac{V}{2}, & N_L + 1 \leq \alpha \leq N_r. \end{cases} \quad (1.69)$$

The current, I_α , carried by the electrons of the sub-band α is given by Eq. (1.53). For simplicity we consider a zero temperature case while the conclusion remains valid at finite temperatures also. So we write

$$I_\alpha = G_0 \sum_{\beta=1}^{N_r} |S_{\alpha\beta}|^2 \{V_\beta - V_\alpha\}. \quad (1.70)$$

Here and below the scattering matrix elements are calculated at $E = \mu_0$.

To calculate the current, I_L , flowing within the left lead we need to sum up the contributions from all the sub-bands belonging to the left lead. These are sub-bands with numbers from 1 until N_L . Therefore, the current I_L is

$$I_L = \sum_{\alpha=1}^{N_L} I_{\alpha}. \quad (1.71)$$

Substituting Eq. (1.70) into Eq. (1.71), we find

$$I_L = V G_0 \sum_{\alpha=1}^{N_L} \sum_{\beta=N_L+1}^{N_r} |S_{\alpha\beta}|^2. \quad (1.72)$$

Calculating in the same way the current I_R flowing into the right lead it is easy to check that $I_R = -I_L$, as expected. Note the equations for the currents $I_{L/R}$ depend only on the transmission probabilities, $|S_{\alpha\beta}|^2$, between the scattering channels belonging to the different leads. Neither intra-sub-bands reflections nor inter-sub-bands transitions within the same lead affect the current.

The conductance, $G = I_L/V$, is

$$G = G_0 \sum_{\alpha=1}^{N_L} \sum_{\beta=N_L+1}^{N_r} |S_{\alpha\beta}|^2. \quad (1.73)$$

Our aim is to show that this quantity is an even function of a magnetic field, $G(H) = G(-H)$. To this end we introduce some generalized reflection coefficients for the reservoirs

$$R_{LL} = \sum_{\alpha=1}^{N_L} \sum_{\beta=1}^{N_L} |S_{\alpha\beta}|^2, \quad R_{RR} = \sum_{\alpha=N_L+1}^{N_r} \sum_{\beta=N_L+1}^{N_r} |S_{\alpha\beta}|^2, \quad (1.74)$$

and transmission coefficients between the reservoirs

$$T_{LR} = \sum_{\alpha=1}^{N_L} \sum_{\beta=N_L+1}^{N_r} |S_{\alpha\beta}|^2, \quad T_{RL} = \sum_{\alpha=N_L+1}^{N_r} \sum_{\beta=1}^{N_L} |S_{\alpha\beta}|^2. \quad (1.75)$$

These coefficients satisfy the following identities,

$$\begin{aligned}
R_{LL} + T_{LR} &= \sum_{\alpha=1}^{N_L} \sum_{\beta=1}^{N_L} |S_{\alpha\beta}|^2 + \sum_{\alpha=1}^{N_L} \sum_{\beta=N_L+1}^{N_r} |S_{\alpha\beta}|^2 \\
&= \sum_{\alpha=1}^{N_L} \sum_{\beta=1}^{N_r} |S_{\alpha\beta}|^2 = \sum_{\alpha=1}^{N_L} 1 = N_L, \\
R_{LL} + T_{RL} &= \sum_{\alpha=1}^{N_L} \sum_{\beta=1}^{N_L} |S_{\alpha\beta}|^2 + \sum_{\alpha=N_L+1}^{N_r} \sum_{\beta=1}^{N_L} |S_{\alpha\beta}|^2 \\
&= \sum_{\beta=1}^{N_L} \sum_{\alpha=1}^{N_r} |S_{\alpha\beta}|^2 = \sum_{\beta=1}^{N_L} 1 = N_L,
\end{aligned}$$

where we used the unitarity of the scattering matrix, $\sum_{\alpha=1}^{N_r} |S_{\alpha\beta}|^2 = 1$, $\sum_{\beta=1}^{N_r} |S_{\alpha\beta}|^2 = 1$. From the above identities it also follows that

$$T_{LR} = T_{RL}. \quad (1.76)$$

Next we use the symmetry conditions, Eq. (1.29), for the scattering matrix elements in the magnetic field and find

$$\begin{aligned}
T_{LR}(-H) &= \sum_{\alpha=1}^{N_L} \sum_{\beta=N_L+1}^{N_r} |S_{\alpha\beta}(-H)|^2 = \sum_{\alpha=1}^{N_L} \sum_{\beta=N_L+1}^{N_r} |S_{\beta\alpha}(H)|^2 \\
&= \sum_{\beta=N_L+1}^{N_r} \sum_{\alpha=1}^{N_L} |S_{\beta\alpha}(H)|^2 = T_{RL}(H).
\end{aligned}$$

Therefore, we have

$$T_{LR}(-H) = T_{RL}(H). \quad (1.77)$$

Combining together Eqs. (1.76) and (1.77) we finally arrive at the required relation

$$\left. \begin{aligned} T_{LR} &= T_{RL} \\ T_{LR}(-H) &= T_{RL}(H) \end{aligned} \right\} \Rightarrow T_{LR}(H) = T_{LR}(-H),$$

which shows that the conductance, $G = G_0 T_{LR}$, of a sample with two quasi-one-dimensional leads is an even function of a magnetic field.

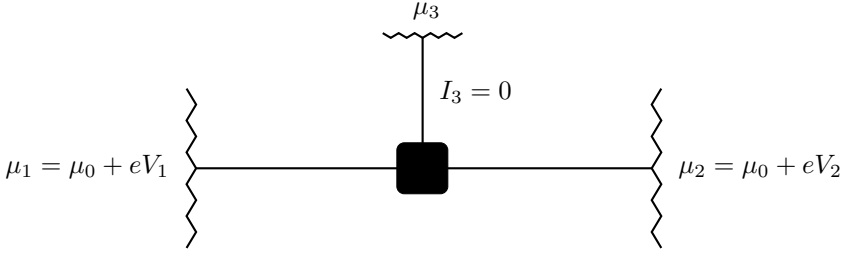


Fig. 1.6 A mesoscopic scatterer with current carrying (1, 2) and potential (3) leads.

1.4.5 Scatterer with a potential contact

The phase coherent system represents an entity whose properties are sometimes quite sensitive to the measurement procedure. If one attaches an additional contact, for instance to measure an electric potential inside the mesoscopic sample, then the current flowing through the system is changed [25, 26].⁵

Let us consider a sample connected to three leads, Fig. 1.6. Two of them, having different electrochemical potentials, $\mu_1 = \mu_0 + eV_1$ and $\mu_2 = \mu_0 + eV_2$, are used to let a current pass through the system. In contrast the third lead acts as a potential contact. As for any potential contacts the current flowing into it is zero, $I_3 = 0$. This condition defines an electrochemical potential, $\mu_3 = \mu_0 + eV_3$, of the third reservoir (which the third lead is connected to) as a function of the bias between the first and the second reservoirs, $V = V_2 - V_1$. One can say that V_3 is a potential of a mesoscopic sample at the point of attachment of the third lead.

Now we calculate the current through the sample. Since $I_3 = 0$ then $I_1 = -I_2$ as for the sample with two leads. Following this analogy we would say that at a given bias V the current depends only on the probability for an electron to go from the first lead to the second lead. However, this is not the case. In the presence of a potential contact (the third lead) the conductance, $G_{12} = I_1/V$, in addition depends on the probability for an electron to be scattered between the current-carrying and the potential leads,

$$I_1 \neq G_0 T_{12} V \quad \Rightarrow \quad G_{12} \neq G_0 T_{12}.$$

⁵In Ref. [22] and mentioned above there is an ingenious idea of how to treat inelastic processes within the scattering approach: It consists in attaching to the sample an additional, fictitious lead. This idea, sometimes essentially modified, see, e.g., Ref. [27], is widely used in the literature due to its simplicity and clarity.

Using Eq. (1.53) we write

$$I_1 = G_0 \left(T_{12}(V_2 - V_1) + T_{13}(V_3 - V_1) \right),$$

$$I_2 = G_0 \left(T_{21}(V_1 - V_2) + T_{23}(V_3 - V_2) \right),$$

$$I_3 = G_0 \left(T_{31}(V_1 - V_3) + T_{32}(V_2 - V_3) \right).$$

From the condition $I_3 = 0$ we find

$$V_3 = \frac{T_{31}V_1 + T_{32}V_2}{T_{31} + T_{32}}.$$

Note the potential $V_3 = 0$ in the symmetric case, namely, if $V_1 = -V_2$ and $T_{31} = T_{32}$. Using the equation for V_3 , we can find the conductance $G_{12} = I_1/(V_2 - V_1)$:

$$G_{12} = G_0 \left\{ T_{12} + \frac{T_{13}T_{32}}{T_{31} + T_{32}} \right\}.$$

In the case of a weak coupling between the potential contact and the sample, $T_{31}, T_{32} \ll T_{12}$, we recover the result for the sample with two leads, $G_{12} \approx G_0 T_{12}$.

1.4.6 Scatterer embedded in a ring

We consider two generic cases: (i) a ring with a magnetic flux Φ and (ii) a ring with scatterer having different transmission amplitudes to the left and to the right. For simplicity we suppose the scatterer located at $x = 0$ to be very thin: Its width w is small compared to the length L of the ring. Then we can choose a wave function on the ring threaded by the magnetic flux Φ , Fig. 1.7, as follows

$$\psi(x) = \left(A e^{ik(x-L)} + B e^{-ikx} \right) e^{i2\pi \frac{x}{L} \frac{\Phi}{\Phi_0}}, \quad 0 \leq x < L. \quad (1.78)$$

The scattering matrix is

$$\hat{S} = \begin{pmatrix} S_{11} & S_{12} \\ S_{21} & S_{22} \end{pmatrix}. \quad (1.79)$$

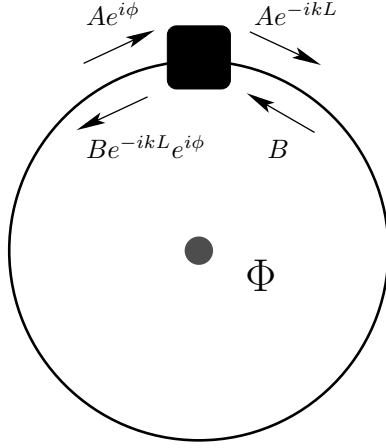


Fig. 1.7 A one-dimensional ring of length L pierced by the magnetic flux Φ with embedded scatterer. A , B are amplitudes of an electron wave function, Eq. (1.78), $\phi = 2\pi\Phi/\Phi_0$.

The scatterer introduces the following boundary conditions ($\alpha = 1$ for $x \rightarrow L - 0$ and $\alpha = 2$ for $x \rightarrow +0$)

$$\begin{aligned}
 Be^{-ikL}e^{i\phi} &= Ae^{i\phi}S_{11} + BS_{12}, \\
 Ae^{-ikL} &= Ae^{i\phi}S_{21} + BS_{22}.
 \end{aligned}
 \tag{1.80}$$

Here we have introduced $\phi = 2\pi\Phi/\Phi_0$. We see that the magnetic flux can be fully incorporated into the non-diagonal scattering matrix elements,

$$S'_{12} = S_{12}e^{-i\phi}, \quad S'_{21} = S_{21}e^{i\phi}.
 \tag{1.81}$$

Therefore, in what follows we will ignore any magnetic flux and only consider the scattering matrix, Eq. (1.79), with $S_{12} \rightarrow S'_{12}$ and $S_{21} \rightarrow S'_{21}$.

1.4.6.1 Spectrum

Now we consider the spectrum of free electrons in a ring with an embedded scatterer. The dispersion equation is defined by the consistency condition

for Eq. (1.80). We rewrite this equation as follows (note that we incorporated ϕ into $S'_{\alpha\beta}$, $\alpha \neq \beta$)

$$AS_{11} - B(e^{-ikL} - S'_{12}) = 0, \quad (1.82)$$

$$A(e^{-ikL} - S'_{21}) - BS_{22} = 0.$$

The consistency condition means that the corresponding determinant is zero,

$$\det \equiv (e^{-ikL} - S'_{21})(e^{-ikL} - S'_{12}) - S_{11}S_{22} = 0. \quad (1.83)$$

To solve it we make the following substitution,

$$S'_{12} = te^{-i\phi}, \quad S'_{21} = te^{i\phi}. \quad (1.84)$$

Next we divide Eq. (1.83) by $S'_{12}S'_{21} = t^2$ and use the equality, $S_{11}S'_{21} = -S'_{12}S_{22}^*$, following from the unitarity of the scattering matrix. Then we arrive at the following

$$\left(\frac{e^{-ikL}}{t} - e^{i\phi}\right)\left(\frac{e^{-ikL}}{t} - e^{-i\phi}\right) = -\frac{|S_{22}|^2}{|S'_{21}|^2}. \quad (1.85)$$

Note the amplitude t can be complex.

Further, since the right hand side (RHS) of Eq. (1.85) is definitely real the left hand side (LHS) of the same equation has to be real as well. After decoupling the real part from the imaginary part we obtain two equations,

$$\left[\operatorname{Re}\left(\frac{e^{-ikL}}{t}\right) - \cos(\phi)\right]^2 + \sin^2(\phi) - \left[\operatorname{Im}\left(\frac{e^{-ikL}}{t}\right)\right]^2 = -\frac{R}{T}, \quad (1.86a)$$

$$\operatorname{Im}\left(\frac{e^{-ikL}}{t}\right) \left[\operatorname{Re}\left(\frac{e^{-ikL}}{t}\right) - \cos(\phi)\right] = 0. \quad (1.86b)$$

Here we introduced $|S_{22}|^2 = R \geq 0$ and $|S'_{12}|^2 \equiv |t|^2 = T \geq 0$. From Eq. (1.86a) we conclude that $\operatorname{Im}(e^{-ikL}/t) \neq 0$ otherwise the LHS of

Eq. (1.86a) would be positive whereas the RHS is strictly negative. Therefore, from Eq. (1.86b) we conclude that the dispersion equation is the following

$$\operatorname{Re}\left(\frac{e^{-ikL}}{t}\right) = \cos(\phi), \quad (1.87)$$

as is well known from the literature [28, 29].

One can check directly that Eq. (1.86a) is consistent with Eq. (1.87).

1.4.6.2 Circulating current

The current carried by an electron in the state with a wave function given by Eq. (1.78) is the following,

$$I = \frac{e\hbar k}{m} (|A|^2 - |B|^2). \quad (1.88)$$

Note the magnetic flux Φ does not enter this equation. Therefore, this equation can be used regardless of whether there is a magnetic flux through the ring or the scattering matrix is merely asymmetric, $S'_{12} \neq S'_{21}$.

To calculate the current, Eq. (1.88), we use both the normalization condition,

$$\int_0^L dx |\psi|^2 \equiv |A|^2 + |B|^2 = 1, \quad (1.89)$$

and one of the equations of the system (1.82), say, the second one,

$$B = A \frac{e^{-ikL} - S'_{21}}{S_{22}} \equiv A \frac{e^{-ikL} - te^{i\phi}}{S_{22}}. \quad (1.90)$$

Substituting Eqs. (1.89) and (1.90) into Eq. (1.88) we find

$$I = \frac{e\hbar k}{mL} \frac{1 - |F|^2}{1 + |F|^2}, \quad |F|^2 = \frac{T}{R} \left| \frac{e^{-ikL}}{t} - e^{i\phi} \right|^2. \quad (1.91)$$

Note at $\phi = 0$, i.e., in the symmetric case $S'_{12} = S'_{21}$, the current, Eq. (1.91), is identically zero, because $|F|^2 = 1$. The latter follows from Eqs. (1.86) and (1.87). The dispersion equation, Eq. (1.87), gives $\operatorname{Re}(e^{-ikL}/t) = 1$. Then at $\phi = 0$ we find from Eq. (1.86a), $[\operatorname{Im}(e^{-ikL}/t)]^2 = R/T$. Therefore, $|F|^2 = T [\operatorname{Im}(e^{-ikL}/t)]^2 / R = TR/(TR) = 1$.

If the scatterer is not symmetric, $S'_{12} \neq S'_{21}$ (i.e., $\phi \neq 0$), then the current is not zero. Using the dispersion equation (1.87), $\text{Re}(e^{-ikL}/t) = \cos(\phi)$, we calculate $|F|^2$

$$\frac{R}{T} |F|^2 = \left[\text{Im} \left(\frac{e^{-ikL}}{t} \right) \right]^2 + \sin^2(\phi) - 2 \text{Im} \left(\frac{e^{-ikL}}{t} \right) \sin(\phi). \quad (1.92)$$

Then from Eqs.(1.86) we find

$$\left[\text{Im} \left(\frac{e^{-ikL}}{t} \right) \right]^2 = \sin^2(\phi) + \frac{R}{T}.$$

Substituting the equation above into Eq. (1.92) and then into Eq. (1.91) we calculate the current

$$I = -\frac{e\hbar k}{mL} \frac{T \sin(\phi)}{T \sin(\phi) + \frac{R}{\sin(\phi) - \text{Im} \left(\frac{e^{-ikL}}{t} \right)}}. \quad (1.93)$$

If we denote $t = it_0 e^{i\chi}$ then the dispersion equation gives: $\sin(kL + \chi) = -t_0 \cos(\phi)$. We write a solution as follows: $k_n L + \chi = \pi n + (-1)^n \arcsin[t_0 \cos(\phi)]$. In this case we calculate, $\text{Im}(e^{-ik_n L}/t) = -\cos(k_n L + \chi)/t_0$. Then the current, Eq. (1.93), reads,

$$I_n = -\frac{e\hbar k_n}{mL} \frac{\sqrt{T} \sin(\phi)}{\sqrt{T} \sin(\phi) + \frac{R}{\sqrt{T} \sin(\phi) + \cos(k_n L + \chi)}}, \quad (1.94)$$

where we use $t_0 = \sqrt{T}$.

Note in the equation above ϕ is either an enclosed magnetic flux or an asymmetry in transmission to the left and to the right, Eq. (1.84), caused, for instance, by the internal magnetic moment. In general R and $T = 1 - R$ can depend on k_n .

Bibliography

- [1] Landauer, R. (1957). Spatial Variation of Currents and Fields Due to Localized Scatterers in Metallic Conduction, *IBM J. Res. Develop.* **1**, pp. 223–231.
- [2] Landauer, R. (1970). Electrical resistance of disordered one-dimensional lattices, *Phil. Mag.* **21**, pp. 863–867.
- [3] Landauer, R. (1975). Residual Resistivity Dipoles, *Z. Phys. B.* **21**, pp. 247–254.
- [4] Büttiker, M. (1990). Scattering theory of thermal and excess noise in open conductors, *Phys. Rev. Lett.* **65**, pp. 2901–2904.
- [5] Büttiker, M. (1992). Scattering theory of current and intensity noise correlations in conductors and wave guides, *Phys. Rev. B* **46**, pp. 12485–12507.
- [6] Büttiker, M. (1993). Capacitance, admittance, and rectification properties of small conductors, *J. Phys. Condensed Matter* **5**, pp. 9361–9378.
- [7] Imry, Y. (1986). Physics of mesoscopic systems, in: Grinstein, G., Mazenko, G. (eds.), *Directions in Condensed Matter Physics* (World Scientific, Singapore), pp. 101–163.
- [8] Imry, Y. (1997). *Introduction to Mesoscopic Physics* (Oxford University Press, New York, Oxford).
- [9] Büttiker, M. and Moskalets, M. (2010). From Anderson Localization to Mesoscopic Physics, in: Abrahams, E. (ed.), *50 Years of Anderson localization* (World Scientific, Singapore), pp. 169–190.
- [10] Beenakker, C. W. J. (1997). Random-matrix theory of quantum transport, *Rev. Mod. Phys.* **69**, N 3, pp. 731–808.
- [11] Fisher, D. S. and Lee, P. A. (1981). Relation between conductivity and transmission matrix, *Phys. Rev. B* **23**, pp. 6851–6854.
- [12] Datta, S. (1995). *Electronic Transport in Mesoscopic Systems* (Cambridge University Press, Cambridge).
- [13] Arrachea, L. and Moskalets, M. (2006). Relation between scattering-matrix and Keldysh formalisms for quantum transport driven by time-periodic fields, *Phys. Rev. B* **74**, 24, p. 245322 (13).
- [14] Landau, L. D. and Lifshits, E. M. (1981). *Quantum Mechanics: Non-Relativistic Theory* (Butterworth-Heinemann, Oxford).

- [15] Landau, L. D. and Lifshits, E. M. (1980). *Statistical Physics, Pt. 1* (Butterworth-Heinemann, Oxford).
- [16] Friedel, J. (1952). The distribution of electrons round impurities in monovalent metals, *Phil. Mag.* **43**, 337, pp. 153–189.
- [17] Taniguchi, T. and Büttiker, M. (1999). Friedel phases and phases of transmission amplitudes in quantum scattering systems, *Phys. Rev. B* **60**, 19, pp. 13814–13823.
- [18] Büttiker, M. (1986). Four-terminal phase-coherent conductance, *Phys. Rev. Lett.* **57**, N 14, pp. 1761–1764.
- [19] Sánchez, D. and Büttiker, M. (2004). Magnetic-field symmetry on nonlinear mesoscopic transport, *Phys. Rev. Lett* **93**, N 10, p. 106802 (4).
- [20] Spivak, B. and Zyuzin, A. (2004). Signature of the Electron-Electron Interaction in the Magnetic-Field Dependence of Nonlinear I-V Characteristics in Mesoscopic Systems, *Phys. Rev. Lett* **93**, N 22, p. 226801 (3).
- [21] Büttiker, M., Imry, Y., and Azbel, M. Y. (1984). Quantum oscillations in one-dimensional normal-metal rings, *Phys. Rev. A* **30**, pp. 1982–1989.
- [22] Büttiker, M. (1985). Small normal-metal loop coupled to an electron reservoir, *Phys. Rev. B* **32**, 3, pp. 1846–1849.
- [23] Griffith, J. S. (1953). A free-electron theory of conjugated molecules. Part 1. Polycyclic hydrocarbons, *Trans. Faraday. Soc.* **49**, pp. 345–351.
- [24] Büttiker, M., Imry, Y., Landauer, R., and Pinhas, S. (1985). Generalized many channel conductance formula with application to small rings, *Phys. Rev. B* **31**, pp. 6207–6215.
- [25] Büttiker, M. (1985). Role of quantum coherence in series resistors, *Phys. Rev. B* **33**, pp. 3020–3026.
- [26] Büttiker, M. (1988). Coherent and sequential tunneling in series barriers, *IBM J. Res. Develop.* **32**, 1, pp. 63–75.
- [27] Beenakker, C. W. J. and Michaelis, B. (2005). Stub model for dephasing in a quantum dot, *J. Phys. A: Math. Gen.* **38**, pp. 10639–10646.
- [28] Anderson, P. W. and Lee, P. A. (1980). The Thouless conjecture for a one-dimensional chain, *Suppl. Prog. Theor. Phys.* **69**, pp. 212–219.
- [29] Cheung, H.-F., Gefen, Y., Riedel, E. K., and Shih, W.-H. (1988). Persistent currents in small one-dimensional metal rings, *Phys. Rev. B* **37**, 11, pp. 6050–6062.
- [30] Landau, L. D. and Lifshits, E. M. (1980). *Statistical Physics, Pt. 2* (Butterworth-Heinemann, Oxford).
- [31] Blanter, Ya. M. and Büttiker, M. (2000). Shot noise in mesoscopic conductors, *Physics Reports* **336**, pp. 1–166.
- [32] Schottky, W. (1918). Über spontane Stromschwankungen in verschiedenen Elektrizitätsleitern, *Ann. Phys. (Leipzig)* **57**, pp. 541–567.
- [33] Kulik, I. O. and Omelyanchouk, A. N. (1984). *Fiz. Nizk. Temp.* **10**, p. 158 [*Sov. J. Low Temp. Phys.* **10**, p. 305].
- [34] Lesovik, G. B. (1989). Excess quantum noise in 2D ballistic point contacts, *Pis'ma v ZhETF* **49**, 9, pp. 513–515 [*JETP Lett.* **49**, 9, pp. 592–594].

- [35] Khlus, V. A. (1987). Current and voltage fluctuations in microjunctions between normal metals and superconductors, *Zh. Eksp. Teor. Fiz.* **93**, p. 2179 [*Sov. Phys. JETP* **66**, p. 1243].
- [36] Gardiner, C. W. and Zoller, P. (2000). *Quantum Noise* (Springer, New York).
- [37] Dirac, P. A. M. (1926). On the theory of quantum mechanics, *Proceedings of the Royal Society, Series A* **112**, pp. 661–677.
- [38] Shirley, J. H. (1965). Solution of the Schrödinger equation with a Hamiltonian periodic in time, *Phys. Rev.* **138**, 4B, pp. 979–987.
- [39] Platero, G. and Aguado, R. (2004). Photon-assisted transport in semiconductor nanostructures, *Physics Reports* **395**, pp. 1–157.
- [40] Moskalets, M. and Büttiker, M. (2002). Floquet scattering theory of quantum pumps, *Phys. Rev. B* **66**, 20, p. 205320 (10).
- [41] Moskalets, M. and Büttiker, M. (2004). Adiabatic quantum pump in the presence of external ac voltages, *Phys. Rev. B* **69**, 20, p. 205316 (12).
- [42] Moskalets, M. and Büttiker, M. (2005). Magnetic-field symmetry of pump currents of adiabatically driven mesoscopic structures, *Phys. Rev. B* **72**, 3, p. 035324 (11).
- [43] Büttiker, M., Thomas, H., and Prêtre, A. (1994). Current partition in multiprobe conductors in the presence of slowly oscillating external potentials, *Z. Phys. B* **94**, pp. 133–137.
- [44] Moskalets, M. and Büttiker, M. (2007). Time-resolved noise of adiabatic quantum pumps, *Phys. Rev. B* **75**, 3, p. 035315 (11).
- [45] Moskalets, M. and Büttiker, M. (2008). Dynamic scattering channels of a double barrier structure, *Phys. Rev. B* **78**, 3, p. 035301 (12).
- [46] Splettstoesser, J., Ol'khovskaya, S., Moskalets, M., and Büttiker, M. (2008). Electron counting with a two-particle emitter, *Phys. Rev. B* **78**, 20, p. 205110 (5).
- [47] Martinez, D. F. and Reichl, L. E. (2001). Transmission properties of the oscillating δ -function potential, *Phys. Rev. B* **64**, 24, p. 245315 (9).
- [48] Sadreev, A. F. and Davlet-Kildeev, K. (2007). Electron transmission through an ac biased quantum point contact, *Phys. Rev. B* **75**, 23, p. 235309 (6).
- [49] Wigner, E. P. (1955). Lower limit for the energy derivative of the scattering phase shift, *Phys. Rev.* **98**, 1, pp. 145–147.
- [50] Smith, F. T. (1960). Lifetime matrix in collision theory, *Phys. Rev.* **118**, 1, pp. 349–356.
- [51] Büttiker, M. and Landauer, R. (1982). Traversal time for tunneling, *Phys. Rev. Lett.* **49**, 23, pp. 1739–1742.
- [52] Büttiker, M. and Landauer, R. (1986). Traversal time for tunneling, *IBM J. Res. Develop.* **30**, 5, pp. 451–454.
- [53] Yafaev, D. R. (1992). *Mathematical Scattering Theory* (AMS).
- [54] de Carvalho, C. A. A. and Nussenzveig, H. M. (2002). Time delay, *Physics Reports* **364**, 2, pp. 83–174.

- [55] Wang, B., Wang, J., and Guo, H. (2003). Current plateaus of nonadiabatic charge pump: Multiphoton assisted processes, *Phys. Rev. B* **68**, 15, p. 155326 (7).
- [56] Wagner, M. (1994). Quenching of resonant transmission through an oscillating quantum well, *Phys. Rev. B* **49**, 23, pp. 16544–16547.
- [57] Wagner, M. (1995). Photon-assisted transmission through an oscillating quantum well: A transfer-matrix approach to coherent destruction of tunneling, *Phys. Rev. A* **51**, 1, pp. 798–808.
- [58] Gutzwiller, M. C. (1971). Periodic orbits and classical quantization conditions, *J. Math. Phys.* **12**, 3, pp. 343–358.
- [59] Jalabert, R. A., Baranger, H. U., and Stone, A. D. (1990). Conductance fluctuations in the ballistic regime: A probe of quantum chaos? *Phys. Rev. Lett.* **65**, 19, pp. 2442–2445.
- [60] Martínez-Mares, M., Lewenkopf, C. H., and Mucciolo, E. R. (2004). Statistical fluctuations of pumping and rectification currents in quantum dots, *Phys. Rev. B* **69**, 8, p. 085301 (12).
- [61] Rahav, S. and Brouwer, P. (2006). Semiclassical theory of a quantum pump, *Phys. Rev. B* **74**, 20, p. 205327 (13).
- [62] Chung, S.-W. V, Moskalets, M., and Samuelsson, P. (2007). Quantum pump driven fermionic Mach–Zehnder interferometer, *Phys. Rev. B* **75**, 11, p. 115332 (10).
- [63] Yang, M. and Li, S.-S. (2004). Device for charge- and spin-pumped current generation with temperature-induced enhancement, *Phys. Rev. B* **70**, 19, p. 195341 (5).
- [64] Yang, M. and Li, S.-S. (2005). Level-oscillation-induced pump effect in a quantum dot with asymmetric constrictions, *Phys. Rev. B* **71**, 12, p. 125307 (4).
- [65] Moskalets, M. V. (1999). Persistent current in a one-dimensional ring with a weak link, *Physica E* **5**, pp. 124–135.
- [66] Moskalets, M. V. (1997). Interference phenomena and ballistic transport in one-dimensional ring, *Fiz. Nizk. Temp.* **23**, 10, pp. 1098–1105 [*Sov. Low Temp. Phys.* **23**, 10, pp. 824–829].
- [67] Moskalets, M. V. (1998). Temperature dependence of the kinetic coefficients of interference ballistic structures, *Zh. Eksp. Teor. Fiz.* **114**, 5, pp. 1827–1835 [*Sov. Phys. JETP* **87**, 5, pp. 991–995].
- [68] Moskalets, M. V. (1998). Temperature-induced current in a one-dimensional ballistic ring with contacts, *Europhys. Lett.* **41**, 2, pp. 189–194.
- [69] Brouwer, P. W. (1998). Scattering approach to parametric pumping, *Phys. Rev. B* **58**, 16, pp. R10135–R10138.
- [70] Thouless, D. J. (1983). Quantization of particle transport, *Phys. Rev. B* **27**, 10, pp. 6083–6087.
- [71] Hekking, F. and Nazarov, Y. V. (1991). Pauli pump for electrons, *Phys. Rev. B* **44**, 16, pp. 9110–9113.
- [72] Spivak, B., Zhou, F., and Beal-Monod, M. T. (1995). Mesoscopic mechanisms of the photovoltaic effect and microwave absorption in granular metals, *Phys. Rev. B* **51**, 19, pp. 13226–13230.

- [73] Stafford, C. A. and Wingreen, N. S. (1996). Resonant photon-assisted tunneling through a double quantum dot: An electron pump from spatial Rabi oscillations, *Phys. Rev. Lett.* **76**, 11, pp. 1916–1919.
- [74] Aleiner, I. L. and Andreev, A. V. (1998). Adiabatic charge pumping in almost open dots, *Phys. Rev. Lett.* **81**, 6, pp. 1286–1289.
- [75] Zhou, F., Spivak, B., and Altshuler, B. (1999). Mesoscopic mechanism of adiabatic charge transport, *Phys. Rev. Lett.* **82**, 3, pp. 608–611.
- [76] Wagner, M. and Sols, F. (1999). Subsea electron transport: pumping deep within the Fermi sea, *Phys. Rev. Lett.* **83**, 21, pp. 4377–4380.
- [77] Simon, S. H. (2000). Proposal for a quantum Hall pump, *Phys. Rev. B* **61**, 24, pp. R16327–R16330.
- [78] Wei, Y., Wang, J., and Guo, H. (2000). Resonance-assisted parametric electron pump, *Phys. Rev. B* **62**, 15, pp. 9947–9950.
- [79] Avron, J. E., Elgart, A., Graf, G. M., and Sadun, L. (2000). Geometry, statistics, and asymptotics of quantum pumps, *Phys. Rev. B* **62**, 16, pp. R10618–R10621.
- [80] Sharma, P. and Chamon, C. (2001). Quantum pump for spin and charge transport in a Luttinger liquid, *Phys. Rev. Lett.* **87**, 9, p. 096401 (17).
- [81] Avron, J. E., Elgart, A., Graf, G. M., and Sadun, L. (2001). Optimal quantum pumps, *Phys. Rev. Lett.* **87**, 23, p. 236601 (4).
- [82] Vavilov, M. G., Ambegaokar, V., and Aleiner, I. L. (2001). Charge pumping and photovoltaic effect in open quantum dots, *Phys. Rev. B* **63**, 19, p. 195313 (12).
- [83] Polianski, M. L. and Brouwer, P. W. (2001). Pumped current and voltage for an adiabatic quantum pump, *Phys. Rev. B* **64**, 7, p. 075304 (6).
- [84] Blaauboer, M. and Heller, E. J. (2001). Statistical distribution of Coulomb blockade peak heights in adiabatically pumped quantum dots, *Phys. Rev. B* **64**, 24, p. 241301(R) (4).
- [85] Tang, C. S. and Chu, C. S. (2001). Nonadiabatic quantum pumping in mesoscopic nanostructures, *Solid State Communications* **120**, pp. 353–357.
- [86] Wang, B., Wang, J., and Guo, H. (2002). Parametric pumping at finite frequency, *Phys. Rev. B* **65**, 7, p. 073306 (4).
- [87] Zhu, S.-L. and Wang, Z. D. (2002). Charge pumping in a quantum wire driven by a series of local time-periodic potentials, *Phys. Rev. B* **65**, 15, p. 155313 (5).
- [88] Moskalets, M. and Büttiker, M. (2002). Dissipation and noise in adiabatic quantum pumps, *Phys. Rev. B* **66**, 3, p. 035306 (9).
- [89] Kim, S. W. (2002). Floquet scattering in parametric electron pumps, *Phys. Rev. B* **66**, 23, p. 235304 (6).
- [90] Moskalets, M. and Büttiker, M. (2003). Hidden quantum pump effects in quantum coherent rings, *Phys. Rev. B* **68**, 7, p. 075303 (8).
- [91] Cohen, D. (2003). Quantum pumping in closed systems, adiabatic transport, and the Kubo formula, *Phys. Rev. B* **68**, 15, p. 155303 (15).
- [92] Moskalets, M. and Büttiker, M. (2003). Quantum pumping: Coherent rings versus open conductors, *Phys. Rev. B* **68**, 16, p. 161311(R) (4).

- [93] Zhou, H.-Q., Cho, S. Y., and McKenzie, R. H. (2003). Gauge fields, geometric phases, and quantum adiabatic pumps, *Phys. Rev. Lett.* **91**, 18, p. 186803 (4).
- [94] Cohen, D. (2003). Quantum pumping and dissipation: From closed to open systems, *Phys. Rev. B* **68**, 20, p. 201303(R) (4).
- [95] Avron, J. E., Elgart, A., Graf, G. M., and Sadun, L. (2004). Transport and dissipation in quantum pumps, *J. of Stat. Phys.* **116**, pp. 425–473.
- [96] Faizabadi, E. and Ebrahimi, F. (2004). Charge pumping in quantum wires, *J. Phys.: Condens. Matter* **16**, pp. 1789–1802.
- [97] Zhou, H.-Q., Lundin, U., Cho, S. Y., and McKenzie, R. H. (2004). Measuring geometric phases of scattering states in nanoscale electronic devices, *Phys. Rev. B* **69**, 11, p. 113308 (4).
- [98] Shin, D. and Hong, J. (2004). Electron transport in the Aharonov–Bohm pump, *Phys. Rev. B* **70**, 7, p. 073301 (4).
- [99] Blaauboer, M. (2005). Quantum pumping and nuclear polarization in the integer quantum Hall regime, *Europhys. Lett.* **69**, 1, pp. 109–115.
- [100] Zhou, H.-Q., Lundin, U., and Cho, S. Y. (2005). Geometric phases of scattering states in a ring geometry: adiabatic pumping in mesoscopic devices, *J. Phys.: Condens. Matter* **17**, pp. 1059–1066.
- [101] Spletstoesser, J., Governale, M., König, J., and Fazio, R. (2005). Adiabatic pumping through interacting quantum dots, *Phys. Rev. Lett.* **95**, 24, p. 246803 (4).
- [102] Governale, M., Taddei, F., Fazio, R., and Hekking, F. W. J. (2005). Adiabatic pumping in a superconductor-normal-superconductor weak link, *Phys. Rev. Lett.* **95**, 25, p. 256801 (4).
- [103] Sela, I. and Cohen, D. (2006). Operating a quantum pump in a closed circuit, *J. Phys. A: Math. Gen.* **39**, pp. 3575–3592.
- [104] Mahmoodian, M. M., Braginsky, L. S., and Entin, M. V. (2006). One-dimensional two-barrier quantum pump with harmonically oscillating barriers: Perturbative, strong-signal, and nonadiabatic regimes, *Phys. Rev. B* **74**, 12, p. 125317 (6).
- [105] Banerjee, S., Mukherjee, A., Rao, S., and Saha, A. (2007). Adiabatic charge pumping through a dot at the junction of N quantum wires, *Phys. Rev. B* **75**, 15, p. 153407 (4).
- [106] Hwang, N. Y., Kim, S. C., Park, P. S., and Eric Yang, S.-R. (2008). Pumping in quantum dots and non-Abelian matrix Berry phases, *Solid State Commun.* **145**, pp. 515–519.
- [107] Qi, X.-L., Hughes T. L., and Zhang, S.-C. (2008). Fractional charge and quantized current in the quantum spin Hall state, *Nature Physics* **4**, pp. 273–276.
- [108] Winkler, N., Governale, M., and König, J. (2009). Diagrammatic real-time approach to adiabatic pumping through metallic single-electron devices, *Phys. Rev. B* **79**, 23, p. 235309 (11).
- [109] Zhu, R. and Chen, H. (2009). Quantum pumping with adiabatically modulated barriers in graphene, *Appl. Phys. Lett.* **95**, 12, p. 122111 (3).

- [110] Prada, E., San-Jose, P., and Schomerus, H. (2009). Quantum pumping in graphene, *Phys. Rev. B* **80**, 24, p. 245414 (5).
- [111] Luo, S.-L. and Wei, Y.-D. (2009). Properties of graphene based parametric pump, *Chin. Phys. Lett.* **26**, 11, p. 117202 (4).
- [112] Zhu, R. and Berakdar, J. (2010). Spin-dependent pump current and noise in an adiabatic quantum pump based on domain walls in a magnetic nanowire, *Phys. Rev. B* **81**, 1, p. 014403 (7).
- [113] Riwar, R.-P. and Splettstoesser, J. (2010). Charge and spin pumping through a double quantum dot, *Phys. Rev. B* **82**, 20, p. 205308 (14).
- [114] Zhang, Q., Chan, K. S., and Lin, Z. (2011). Spin current generation by adiabatic pumping in monolayer graphene, *Appl. Phys. Lett.* **98**, 3, p. 032106 (3).
- [115] Sinitsyn, N. A. (2009). The stochastic pump effect and geometric phases in dissipative and stochastic systems, *J. Phys. A: Math. Theor.* **42**, 19, p. 193001 (33).
- [116] Switkes, M., Marcus, C. M., Campman, K., and Gossard, A. C. (1999). An adiabatic quantum electron pump, *Science* **283**, pp. 1905–1908.
- [117] Höhberger, E. M., Lorke, A., Wegscheider, W., and Bichler, M. (2001). Adiabatic pumping of two-dimensional electrons in a ratchet-type lateral superlattice, *Appl. Phys. Lett.* **78**, 19, pp. 2905–2907.
- [118] Watson, S. K., Potok, R. M., Marcus, C. M., and Umansky, V. (2003). Experimental realization of a quantum spin pump, *Phys. Rev. Lett.* **91**, N 25, p. 258301 (4).
- [119] Liu, K.-M., Umansky, V., and Hsu, S.-Y. (2010). Time dependent electric fields generated DC currents in a large gate-defined open dot, *Jap. J. Appl. Phys.* **49**, p. 114001 (4).
- [120] Niu, Q. (1990). Towards a quantum pump of electric charges, *Phys. Rev. Lett.* **64**, 15, pp. 1812–1815.
- [121] Liu, C. and Niu, Q. (1993). Nonadiabatic effect in a quantum charge pump, *Phys. Rev. B* **47**, 19, pp. 13031–13034.
- [122] Makhlin, Y. and Mirlin, A. D. (2001). Counting statistics for arbitrary cycles in quantum pumps, *Phys. Rev. Lett.* **87**, 27, p. 276803 (4).
- [123] Levinson, Y., Entin-Wohlman, O., and Wölfle, P. (2001). Pumping at resonant transmission and transferred charge quantization, *Physica A* **302**, pp. 335–344.
- [124] Kashcheyevs, V., Aharony, A., and Entin-Wohlman, O. (2004). Resonance approximation and charge loading and unloading in adiabatic quantum pumping, *Phys. Rev. B* **69**, 19, p. 195301 (9).
- [125] Blumenthal, M. D., Kaestner, B., Li, L., Giblin, S., Janssen, T. J. B. M., Pepper, M., Anderson, D., Jones, G., and Ritchie, D. A. (2007). Gigahertz quantized charge pumping, *Nature Physics* **3**, pp. 343–347.
- [126] Fujiwara, A., Nishiguchi, K., and Ono, Y. (2008). Nanoampere charge pump by single-electron ratchet using silicon nanowire metal-oxide-semiconductor field-effect transistor, *Appl. Phys. Lett.* **92**, 4, p. 042102 (3).

- [127] Kaestner, B., Kashcheyevs, V., Amakawa, S., Blumenthal, M. D., Li, L., Janssen, T. J. B. M., Hein, G., Pierz, K., Weimann, T., Siegner, U., and Schumacher, H. W. (2008). Single-parameter nonadiabatic quantized charge pumping, *Phys. Rev. B* **77**, 15, p. 153301 (4).
- [128] Miyamoto, S., Nishiguchi, K., Ono, Y., Itoh, K. M., and Fujiwara, A. (2010). Resonant escape over an oscillating barrier in a single-electron ratchet transfer, *Phys. Rev. B* **82**, 3, p. 033303 (4).
- [129] Fève, G., Mahé, A., Berroir, J.-M., Kontos, T., Plaças, B., Glattli, D. C., Cavanna, A., Etienne, B., and Jin, Y. (2007). An on-demand coherent single-electron source, *Science* **316**, pp. 1169–1172.
- [130] Kouwenhoven, L. P., Johnson, A. T., van der Vaart, N. C., Harmans, C. J. P. M., and Foxon, C. T. (1991). Quantized current in a quantum-dot turnstile using oscillating tunnel barriers, *Phys. Rev. Lett.* **67**, 12, pp. 1626–1629.
- [131] Keller, M. W., Martinis, J. M., Zimmerman, N. M., and Steinbach, A. H. (1996). Accuracy of electron counting using a 7-junction electron pump, *Appl. Phys. Lett.* **69**, 12, pp. 1804–1806.
- [132] Berg, E., Levin, M., and Altman, E. (2011). Quantized pumping and topology of the phase diagram for a system of interacting bosons, *Phys. Rev. Lett.* **106**, 11, p. 110405 (4).
- [133] Niu, Q. (1986). Quantum adiabatic particle transport, *Phys. Rev. B* **34**, 8, pp. 5093–5100.
- [134] Onoda, S., Murakami, S., and Nagaosa, N. (2004). Topological nature of polarization and charge pumping in ferroelectrics, *Phys. Rev. Lett.* **93**, 16, p. 167602 (4).
- [135] Fu, L. and Kane, C. L. (2006). Time reversal polarization and a Z2 adiabatic spin pump, *Phys. Rev. B* **64**, 19, p. 195312 (13).
- [136] Chern, C. H., Onoda, S., Murakami, S., and Nagaosa, N. (2007). Quantum charge pumping and electric polarization in Anderson insulators, *Phys. Rev. B* **76**, 3, p. 035334 (15).
- [137] Leone, R., Lévy, L. P., and Lafarge, P. (2008). Cooper-pair pump as a quantized current source, *Phys. Rev. Lett.* **100**, 11, p. 117001 (4).
- [138] Teo, J. C. Y. and Kane, C. L. (2010). Topological defects and gapless modes in insulators and superconductors, *Phys. Rev. B* **82**, 11, p. 115120 (26).
- [139] Meidan, D., Micklitz, T., and Brouwer, P. W. (2010). Optimal topological spin pump, *Phys. Rev. B* **82**, 16, p. 161303(R) (4).
- [140] Maruyama, I. and Hatsugai, Y. (2009). Non-adiabatic effect on Laughlins argument of the quantum Hall effect, *J. Phys.: Conf. Ser.* **150**, 2, p. 022055 (4).
- [141] Graf, G. M. and Ortelli, G. (2008). Comparison of quantization of charge transport in periodic and open pumps, *Phys. Rev B* **77**, 3, p. 033304 (3).
- [142] Bräunlich, G., Graf, G. M., and Ortelli, G. (2010). Equivalence of topological and scattering approaches to quantum pumping, *Commun. Math. Phys.* **295**, pp. 243–259.

- [143] Reydellet, L.-H., Roche, P., Glattli, D. C., Etienne, B., and Jin, Y. (2003). Quantum partition noise of photon-created electron-hole pairs, *Phys. Rev. Lett.* **90**, 17, p. 176803 (4).
- [144] Rychkov, V. S., Polianski, M. L., and Büttiker, M. (2005). Photon-assisted electron-hole shot noise in multiterminal conductors, *Phys. Rev. B* **72**, 15, p. 155326 (9).
- [145] Polianski, M. L., Samuelsson, P., and Büttiker, M. (2005). Shot noise of photon-excited electron-hole pairs in open quantum dots, *Phys. Rev. B* **72**, 16, p. 161302(R) (4).
- [146] Moskalets, M. and Büttiker, M. (2001). Effect of inelastic scattering on parametric pumping, *Phys. Rev. B* **64**, 20, p. 201305(R) (4).
- [147] Büttiker, M. and Moskalets, M. (2006). Scattering theory of dynamic electrical transport, *Lecture Notes in Physics* **690**, p. 33–44.
- [148] Cremers, J. N. H. J. and Brouwer, P. W. (2002). Dephasing in a quantum pump, *Phys. Rev. B* **65**, 11, p. 115333 (7).
- [149] Wagner, M. (2000). Probing Pauli blocking factors in quantum pumps with broken time-reversal symmetry, *Phys. Rev. Lett.* **85**, 1, pp. 174–177.
- [150] Kohler, S., Lehmann, J., and Hänggi, P. (2005). Driven quantum transport on the nanoscale, *Physics Reports* **406**, pp. 379–443.
- [151] DiCarlo, L., Marcus, C. M., and Harris, J. S., Jr. (2003). Photocurrent, rectification, and magnetic field symmetry of induced current through quantum dots, *Phys. Rev. Lett.* **91**, 24, p. 246804 (4).
- [152] Vavilov, M. G., DiCarlo, L., and Marcus, C. M. (2005). Photovoltaic and rectification currents in quantum dots, *Phys. Rev. B* **71**, 24, p. 241309(R) (4).
- [153] Arrachea, L. (2005). Green-function approach to transport phenomena in quantum pumps, *Phys. Rev. B* **72**, 12, p. 125349 (11).
- [154] Foa Torres, L. E. F. (2005). Mono-parametric quantum charge pumping: Interplay between spatial interference and photon-assisted tunneling, *Phys. Rev. B* **72**, 24, p. 245339 (7).
- [155] Agarwal, A. and Sen, D. (2007). Non-adiabatic charge pumping by an oscillating potential, *Phys. Rev. B* **76**, 23, p. 235316 (8).
- [156] Cavaliere, F., Governale, M., and König, J. (2009). Nonadiabatic pumping through interacting quantum dots, *Phys. Rev. Lett.* **103**, 13, p. 136801 (4).
- [157] Gu, Y., Yang, Y. H., Wang, J., and Chan, K. S. (2009). Single-parameter charge pump in a zigzag graphene nanoribbon, *J. Phys. Condens. Matter* **21**, p. 405301 (6).
- [158] Soori, A. and Sen, D. (2010). Nonadiabatic charge pumping by oscillating potentials in one dimension: Results for infinite system and finite ring, *Phys. Rev. B* **82**, 11, p. 115432 (15).
- [159] Kaestner, B., Kashcheyevs, V., Hein, G., Pierz, K., Siegner, U., and Schumacher, H. W. (2008). Robust single-parameter quantized charge pumping, *Appl. Phys. Lett.* **92**, 19, p. 192106 (3).

- [160] Wright, S. J., Blumenthal, M. D., Gumbs, G., Thorn, A. L., Pepper, M., Janssen, T. J. B. M., Holmes, S. N., Anderson, D., Jones, G. A. C., Nicoll, C. A., and Ritchie, D. A. (2008). Enhanced current quantization in high-frequency electron pumps in a perpendicular magnetic field, *Phys. Rev. B* **78**, 23, p. 233311 (4).
- [161] Kaestner, B., Leich, C., Kashcheyevs, V., Pierz, K., Siegner, U., and Schumacher, H. W. (2009). Single-parameter quantized charge pumping in high magnetic fields, *Appl. Phys. Lett.* **94**, 1, p. 012106 (3).
- [162] Wright, S. J., Blumenthal, M. D., Pepper, M., Anderson, D., Jones, G. A. C., Nicoll, C. A., and Ritchie, D. A. (2009). Parallel quantized charge pumping, *Phys. Rev. B* **80**, 11, p. 113303 (3).
- [163] Giblin, S. P., Wright, S. J., Fletcher, J. D., Kataoka, M., Pepper, M., Janssen, T. J. B. M., Ritchie, D. A., Nicoll, C. A., Anderson, D., and Jones, G. A. C. (2010). An accurate high-speed single-electron quantum dot pump, *New J. Phys.* **12**, p. 073013 (8).
- [164] Mirovsky, P., Kaestner, B., Leicht, C., Welker, A. C., Weimann, T., Pierz, K., and Schumacher, H. W. (2010). Synchronized single electron emission from dynamical quantum dots, *Appl. Phys. Lett.* **97**, 25, p. 252104 (3).
- [165] Qi, X.-L. and Zhang, S.-C. (2009). Field-induced gap and quantized charge pumping in a nanoscale helical wire, *Phys. Rev. B* **79**, 23, p. 235442 (6).
- [166] Zólyomi, V., Oroszlány, L., and Lambert, C. J. (2009). Quantum pumps formed of double walled carbon nanotubes, *Phys. Status Solidi B* **246**, 11-12, pp. 2650–2653.
- [167] Oroszlány, L., Zólyomi, V., and Lambert, C. J. (2010). Carbon nanotube Archimedes screws, *ACS Nano* **4**, 12, pp. 7363–7366.
- [168] Jääskeläinen, M., Corvino, F., Search, C. P., and Fessatidis, V. (2008). Quantum pumping of electrons by a moving modulated potential, *Phys. Rev. B* **77**, 15, p. 155319 (8).
- [169] Das, K. K. and Opatrný, T. (2010). What is quantum in quantum pumping: The role of phase and asymmetries, *Phys. Lett. A* **374**, pp. 485–490.
- [170] Prêtre, A., Thomas, H., and Büttiker, M. (1996). Dynamic admittance of mesoscopic conductors: Discrete-potential model, *Phys. Rev. B* **54**, 11, pp. 8130–8143.
- [171] Brouwer, P. W. and Büttiker, M. (1997). Charge-relaxation and dwell time in the fluctuating admittance of a chaotic cavity, *Europhys. Lett.* **37**, 7, pp. 441–446.
- [172] Büttiker, M. (2002). Charge densities and charge noise in mesoscopic conductors, *Pramana-J. Phys.* **58**, 2, pp. 241–257.
- [173] Jauho, A.-P., Wingreen, N. S., and Meir, Y. (1994). Time-dependent transport in interacting and noninteracting resonant-tunneling systems, *Phys. Rev. B* **50**, 8, pp. 5528–5544.
- [174] Pedersen, M. H. and Büttiker, M. (1998). Scattering theory of photon-assisted electron transport, *Phys. Rev. B* **58**, 19, pp. 12993–13006.
- [175] Brouwer, P. W. (2001). Rectification of displacement currents in an adiabatic electron pump, *Phys. Rev. B* **63**, 12, p. 121303(R) (2).

- [176] Arrachea, L. (2005). Symmetry and environment effects on rectification mechanisms in quantum pumps, *Phys. Rev. B* **72**, 12, p. 121306(R) (4).
- [177] Benjamin, C. (2006). Detecting a true quantum pump effect, *Eur. Phys. J. B* **52**, pp. 403–410.
- [178] Moskalets, M. and Büttiker, M. (2004). Floquet scattering theory for current and heat noise in large amplitude adiabatic pumps, *Phys. Rev. B* **70**, 24, p. 245305 (15).
- [179] Polianski, M. L., Vavilov, M. G., and Brouwer, P. W. (2002). Noise through quantum pumps, *Phys. Rev. B* **65**, 24, p. 245314 (9).
- [180] Polianski, M. L. and Brouwer, P. W. (2003). Scattering matrix ensemble for time-dependent transport through a chaotic quantum dot, *J. Phys. A: Math. Gen.* **36**, pp. 3215–3236.
- [181] Vavilov, M. G. (2005). Quantum chaotic scattering in time-dependent external fields: random matrix approach, *J. Phys. A: Math. Gen.* **38**, pp. 10587–10611.
- [182] Levitov, L. S. and Lesovik, G. B. (1993). Charge distribution in quantum shot noise, *Pis'ma v ZhETF* **58**, 3, pp. 225–230 [*JETP Lett.* **58**, 3, pp. 230–235].
- [183] Ivanov, D. A. and Levitov, L. S. (1993). Statistics of charge fluctuations in quantum transport in an alternating field, *Pis'ma v ZhETF* **58**, 6, pp. 450–456 [*JETP Lett.* **58**, 6, pp. 461–468].
- [184] Esposito, M., Harbola, U., and Mukamel, S. (2009). Nonequilibrium fluctuations, fluctuation theorems, and counting statistics in quantum systems, *Rev. Mod. Phys.* **81**, 4, pp. 1665–1702.
- [185] Andreev, A. and Kamenev, A. (2000). Counting statistics of an adiabatic pump, *Phys. Rev. Lett.* **85**, 6, pp. 1294–1297.
- [186] Levitov, L. S. Counting statistics of charge pumping in an open system, cond-mat/0103617 (unpublished).
- [187] Andreev, A. V. and Mishchenko, E. G. (2001). Full counting statistics of a charge pump in the Coulomb blockade regime, *Phys. Rev. B* **64**, 23, p. 233316 (4).
- [188] Muzykantskii, B. A. and Adamov, Y. (2003). Scattering approach to counting statistics in quantum pumps, *Phys. Rev. B* **68**, 15, p. 155304 (9).
- [189] Camalet, S., Lehmann, J., Kohler, J., and Hänggi, P. (2003). Current noise in ac-driven nanoscale conductors, *Phys. Rev. Lett.* **90**, 21, p. 210602.
- [190] Abanov, A. G. and Ivanov, D. A. (2009). Factorization of quantum charge transport for noninteracting fermions, *Phys. Rev. B* **79**, 20, p. 205315 (9).
- [191] Ivanov, D. A. and Abanov, A. G. (2010). Phase transitions in full counting statistics for periodic pumping, *Europhys. Lett.* **92**, 3, p. 37008 (5).
- [192] Wang, B., Wang, J., and Guo, H. (2004). Shot noise of spin current, *Phys. Rev. B* **69**, 15, p. 153301 (4).
- [193] Camalet, S., Kohler, J., and Hänggi, P. (2004). Shot noise control in ac-driven nanoscale conductors, *Phys. Rev. B* **70**, 15, p. 155326.
- [194] Strass, M., Hänggi, P., and Kohler, S. (2005). Nonadiabatic electron pumping: Maximal current with minimal noise, *Phys. Rev. Lett.* **95**, 13, p. 130601 (4).

- [195] Li, C., Yu, Y., Wei, Y., and Wang, J. (2007). Statistical analysis for current fluctuations in a disordered quantum pump, *Phys. Rev. B* **76**, 23, p. 235305 (5).
- [196] Maire, N., Hohls, F., Kaestner, B., Pierz, K., Schumacher, H. W., and Haug, R. J. (2008). Noise measurement of a quantized charge pump, *Appl. Phys. Lett.* **92**, 8, p. 082112 (3).
- [197] Samuelsson, P. and Büttiker, M. (2005). Dynamic generation of orbital quasiparticle entanglement in mesoscopic conductors, *Phys. Rev. B* **71**, 24, p. 245317 (5).
- [198] Beenakker, C. W. J., Titov, M., and Trauzettel, B. (2005). Optimal spin-entangled electron-hole pair pump, *Phys. Rev. Lett.* **94**, 18, p. 186804 (4).
- [199] Moskalets, M. and Büttiker, M. (2006). Multiparticle correlations of an oscillating scatterer, *Phys. Rev. B* **73**, 12, p. 125315 (6).
- [200] Das, K. K., Kim, S., and Mizel, A. (2006). Controlled flow of spin-entangled electrons via adiabatic quantum pumping, *Phys. Rev. Lett.* **97**, 9, p. 096602 (4).
- [201] Beenakker, C. W. J. (2005). Electron-hole entanglement in the Fermi sea, in *Quantum Computers, Algorithms and Chaos, Proceedings of the International School of Physics Enrico Fermi, Course CLXII, Varenna, 2005* (IOS, Amsterdam, 2006), pp. 307–347; see also e-print arXiv:cond-mat/0508488.
- [202] Abrikosov, A. A. (1988). *Fundamentals of the Theory of Metals* (Elsevier Science, Amsterdam).
- [203] Arrachea, L. and Moskalets, M. (2010). Energy transport and heat production in quantum engines, in: Sattler, K. D. (ed.), *Handbook of Nanophysics: Nanomedicine and Nanorobotics* (CRC Press, Taylor & Francis Group).
- [204] Wang, B. and Wang, J. (2002). Heat current in a parametric quantum pump, *Phys. Rev. B* **66**, 12, p. 125310 (4).
- [205] Wei, Y., Wan, L., Wang, B., and Wang, J. (2004). Heat current and spin current through a carbon-nanotube-based molecular quantum pump, *Phys. Rev. B* **70**, 4, p. 045418 (9).
- [206] Fransson, J. and Galperin, M. (2010). Inelastic scattering and heating in a molecular spin pump, *Phys. Rev. B* **81**, 7, p. 075311 (8).
- [207] Humphrey, T. E., Linke, H., and Newbury, R. (2001). Pumping heat with quantum ratchets, *Physica E* **11**, pp. 281–286.
- [208] Segal, D. and Nitzan, A. (2006). Molecular heat pump, *Phys. Rev. E* **73**, 02, p. 026109 (9).
- [209] Arrachea, L., Moskalets, M., and Martin-Moreno, L. (2007). Heat production and energy balance in nanoscale engines driven by time-dependent fields, *Phys. Rev. B* **75**, 24, p. 245420 (5).
- [210] Rey, M., Strass, M., Kohler, S., Hänggi, P., and Sols, F. (2007). Nonadiabatic electron heat pump, *Phys. Rev. B* **76**, 8, p. 085337 (4).
- [211] Cuansing, E. C. and Wang, J.-S. (2010). Tunable heat pump by modulating the coupling to the leads, *Phys. Rev. B* **82**, 2, p. 021116 (9).
- [212] Chamon, C., Mucciolo, E. R., Arrachea, L., and Capaz, R. B. (2011). Heat pumping in nanomechanical systems, *Phys. Rev. Lett.* **106**, 13, p. 135504 (4).

- [213] Bauer, G. E. W., Bretzel, S., Brataas, A., and Tserkovnyak, Y. (2010). Nanoscale magnetic heat pumps and engines, *Phys. Rev. B* **81**, 2, p. 024427 (11).
- [214] Büttiker, M., Thomas, H., and Prêtre, A. (1993). Mesoscopic capacitors, *Phys. Lett. A* **180**, 4,5, pp. 364–369.
- [215] Moskalets, M. and Büttiker, M. (2009). Heat production and current noise for single- and double-cavity quantum capacitors, *Phys. Rev. B* **80**, 8, p. 081302 (4).
- [216] Gabelli, J., Fève, G., Berroir, J.-M., Plaçais, B., Cavanna, A., Etienne, B., Jin, Y., and Glattli, D. C. (2006). Violation of Kirchhoff’s Laws for a coherent RC circuit, *Science* **313**, pp. 499–502.
- [217] Ol’khovskaya, S., Splettstoesser, J., Moskalets, M., and Büttiker, M. (2008). Shot noise of a mesoscopic two-particle collider, *Phys. Rev. Lett.* **101**, 16, p. 166802 (4).
- [218] Splettstoesser, J., Moskalets, M., and Büttiker, M. (2009). Two-particle non-local Aharonov–Bohm effect from two single-particle emitters, *Phys. Rev. Lett.* **103**, 7, p. 076804 (4).
- [219] Mahé, A., Parmentier, F. D., Bocquillon, E., Berroir, J.-M., Glattli, D. C., Kontos, T., Plaçais, B., Fève, G., Cavanna, A., and Jin, Y. (2010). Current correlations of an on-demand electron source as an evidence of single particle emission, *Phys. Rev. B* **82**, 20, p. 201309 (4).
- [220] Albert, M., Flindt, C., and Büttiker, M. (2010). Accuracy of the quantum capacitor as a single-electron source, *Phys. Rev. B* **82**, 4, p. 041407(R) (4).
- [221] Moskalets, M., Samuelsson, P., and Büttiker, M. (2008). Quantized dynamics of a coherent capacitor, *Phys. Rev. Lett.* **100**, 8, p. 086601 (4).
- [222] Fertig, H. A. (1988). Semiclassical description of a two-dimensional electron in a strong magnetic field and an external potential, *Phys. Rev. B* **38**, 2, pp. 996–1015.
- [223] Chung, V. S.-W., Samuelsson, P. and Büttiker, M. (2005). Visibility of current and shot noise in electrical Mach–Zehnder and Hanbury Brown Twiss interferometers, *Phys. Rev. B* **72**, 12, p. 125320 (13).
- [224] van der Vaart, N. C., van de Ruyter, Steveninck, M. P., Kouwenhoven, L. P., Johnson, A. T., Nazarov, Y. V., Harmans, C. J. P. M., and Foxon, C. T. (1994). Time-resolved tunneling of single electrons between Landau levels in a quantum dot, *Phys. Rev. Lett.* **73**, 2, pp. 320–323.
- [225] McClure, D. T., Zhang, Y., Rosenow, B., Levenson-Falk, E. M., Marcus, C. M., Pfeiffer, L. N., and West, K. W. (2009). Edge-state velocity and coherence in a quantum Hall Fabry–Pérot interferometer. *Phys. Rev. Lett.* **103**, 20, p. 206806 (4).
- [226] Stern, F. (1972). Low temperature capacitance of inverse silicon MOS devices in high magnetic fields, *IBM Research Report*, RC 3758.
- [227] Smith, T. P., Goldberg, B. B., Stiles, P. J., and Heiblum, M. (1985). Direct measurement of the density of states of a two-dimensional electron gas, *Phys. Rev. B* **32**, 4, pp. 2696–2699.

- [228] Smith, T. P., Wang, W. I., and Stiles, P. J. (1986). Two-dimensional density of states in the extreme quantum limit, *Phys. Rev. B* **34**, 4, pp. 2995–2998.
- [229] Luryi, S. (1987). Quantum capacitance devices, *Appl. Phys. Lett.* **52**, 6, pp. 501–503.
- [230] Lafarge, P., Pothier, H., Williams, E. R., Esteve, D., Urbina, C., and Devoret, M. H. (1991). Direct observation of macroscopic charge quantization, *Z. Phys. B – Condensed Matter* **85**, pp. 327–332.
- [231] Ashoori, R. C., Stormer, H. L., Weiner, J. S., Pfeiffer, L. N., Pearton, S. J., Baldwin, K. W., and West, K. W. (1992). Single-electron capacitance spectroscopy of discrete quantum levels, *Phys. Rev. Lett.* **68**, 20, pp. 3088–3091.
- [232] Field, M., Smith, C. G., Pepper, M., Brown, K. M., Linfield, E. H., Grimshaw, M. P., Ritchie, D. A., and Jones, G. A. C. (1996). Coulomb blockade as a noninvasive probe of local density of states, *Phys. Rev. Lett.* **77**, 2, pp. 350–353.
- [233] Büttiker, M. (2000). Time-dependent transport in mesoscopic structures, *J. Low Temp. Phys.* **118**, 5/6, pp. 519–542.
- [234] Nigg, S. E., Lopez, R. and Büttiker, M. (2006). Mesoscopic charge relaxation, *Phys. Rev. Lett.* **97**, 20, p. 206804 (4).
- [235] Ringel, Z., Imry, Y., and Entin-Wohlman, O. (2008). Delayed currents and interaction effects in mesoscopic capacitors, *Phys. Rev. B* **78**, 16, p. 165304 (8).
- [236] Mora, C. and Le Hur, K. (2010). Universal resistances of the quantum RC circuit, *Nature Physics* **6**, pp. 697–701.
- [237] Hamamoto, Y., Jonckheere, T., Kato, T., and Martin, T. (2010). Dynamic response of a mesoscopic capacitor in the presence of strong electron interactions, *Phys. Rev. B* **81**, 15, p. 153305 (4).
- [238] Nigg, S. E. and Büttiker, M. (2008). Quantum to classical transition of the charge relaxation resistance of a mesoscopic capacitor, *Phys. Rev. B* **77**, 8, p. 085312 (10).
- [239] Fu, Y. and Dudley, S. C. (1993). Quantum inductance within linear response theory, *Phys. Rev. Lett.* **70**, 1, pp. 65–68.
- [240] Gabelli, J., Fève, G., Kontos, T., Berroir, J.-M., Plaçais, B., Glattli, D.C., Etienne, B., Jin, Y., and Büttiker, M. (1997). Relaxation time of a chiral quantum R-L circuit, *Phys. Rev. Lett.* **98**, 16, p. 166806 (4).
- [241] Wang, J., Wang, B., and Guo, H. (2007). Quantum inductance and negative electrochemical capacitance at finite frequency in a two-plate quantum capacitor, *Phys. Rev. B* **75**, 15, p. 155336 (5).
- [242] Begliarbakov, M., Strauf, S., and Search, C. P. (2011). Quantum inductance and high frequency oscillators in graphene nanoribbons, *Nanotechnology* **22**, 16, p. 165203 (8).
- [243] Christen, T. and Büttiker, M. (1996). Low-frequency admittance of quantized Hall conductors, *Phys. Rev. B* **53**, 4, pp. 2064–2072.

- [244] Keeling, J., Shytov, A. V., and Levitov, L. S. (2008). Coherent particle transfer in an on-demand single-electron source, *Phys. Rev. Lett.* **101**, 19, p. 196404 (4).
- [245] Sasaoka, K., Yamamoto, T., and Watanabe, S. (2010). Single-electron pumping from a quantum dot into an electrode, *Appl. Phys. Lett.* **96**, 10, p. 102105 (3).
- [246] Splettstoesser, J., Governale, M., König, J., and Büttiker, M. (2010). Charge and spin dynamics in interacting quantum dots, *Phys. Rev. B* **81**, 16, p. 165318 (5).
- [247] Breit, G. and Wigner, E. (1934). Capture of slow neutrons, *Phys. Rev.* **49**, 7, pp. 519–531.
- [248] Battista, F. and Samuelsson, P. (2011). Proposal for non-local electron-hole turnstile in the Quantum Hall regime, *Phys. Rev. B* **83**, 12, p. 125324 (5).
- [249] Keeling, J., Klich, I., and Levitov, L. S. (2006). Minimal excitation states of electrons in one-dimensional wires, *Phys. Rev. Lett.* **97**, 11, p. 116403 (4).
- [250] Sherkunov, Y., Zhang, J., d’Ambrumenil, N., and Muzykantskii, B. (2009). Optimal electron entangler and single-electron source at low temperatures, *Phys. Rev. B* **80**, 4, p. 041313(R) (4).
- [251] Hong, C. K., Ou, Z. Y., and Mandel, L. (1987). Measurements of subpicosecond time intervals between two photons by interference, *Phys. Rev. Lett.* **59**, 18, pp. 2044–2046.
- [252] Glauber, R. J. (1963). The quantum theory of optical coherence, *Phys. Rev.* **130**, 6, pp. 2529–2539.
- [253] Moskalets, M. and Büttiker, M. (2011). Spectroscopy of electron flows with single- and two-particle emitters, *Phys. Rev. B* **83**, 3, p. 035316 (11).
- [254] Bell, J. S. (1966). On the problem of hidden variables in quantum mechanics, *Rev. Mod. Phys.* **38**, 3, pp. 447–452.
- [255] Martin, T. and Landauer, R. (1992). Wave-packet approach to noise in multichannel mesoscopic systems, *Phys. Rev. B* **45**, 4, pp. 1742–1755.
- [256] Büttiker, M. (1992). Role of scattering amplitudes in frequency-dependent current fluctuations in small conductors, *Phys. Rev. B* **45**, 7, pp. 3807–3810.
- [257] Henny, M., Oberholzer, S., Strunk, C., Heinzl, T., Ensslin, K., Holland, M., and Schönberger, C. (1999). The Fermionic Hanbury Brown and Twiss Experiment, *Science* **284**, pp. 296–298.
- [258] Oliver, W. D., Kim, J., Liu, R. C., and Yamamoto, Y. (1999). Hanbury Brown and Twiss-Type Experiment with electrons, *Science* **284**, pp. 299–301.
- [259] Samuelsson, P., Sukhorukov, E. V., and Büttiker, M. (2004). Two-particle Aharonov–Bohm effect and entanglement in the electronic Hanbury Brown Twiss setup, *Phys. Rev. Lett.* **92**, 2, pp. 026805 (4).
- [260] Samuelsson, P., Neder, I., and Büttiker, M. (2009). Reduced and projected two-particle entanglement at finite temperatures, *Phys. Rev. Lett.* **102**, 10, pp. 106804 (4).

- [261] Neder, I., Ofek, N., Chung, Y., Heiblum, M., Mahalu, D., and Umansky, V. (2007). Interference between two indistinguishable electrons from independent sources, *Nature* **448**, pp. 333–337.
- [262] Splettstoesser, J., Samuelsson, P., Moskalets, M., and Büttiker, M. (2010). Two-particle Aharonov–Bohm effect in electronic interferometers, *J. Phys. A: Math. Theor.* **43**, 35, p. 354027 (9).

Index

- adiabaticity, 80
 - parameter, 80
 - linear response regime, 210
 - non-linear regime, 210
- approximation
 - single-electron, 9
- capacitance
 - differential, 198
- conductance
 - frequency dependent, 191
 - frozen, 158
 - matrix elements, 18
 - quantum, 18
 - thermoelectric, 20
- current decay time, 200
- current spectral density, 120
- density of states, 11
 - dynamic, 197
 - frozen
 - chiral ring, 197
 - partial
 - frozen, 131
 - stationary, 194
- distribution function
 - equilibrium, 13
 - non-equilibrium, 15, 113
- equivalent electric circuit, 192
 - parameters
 - high temperatures, 192
 - zero temperature, 193
- equivalent electrical circuit
 - non-linear regime, 197
 - parameters
 - non-linear regime, 198
- heat flow
 - generated, 169
 - quantized emission regime, 211
 - transferred, 170
- mesoscopic capacitor, 175
- noise
 - shot, 36, 46
 - photon-assisted, 159
 - quantized, 212
 - suppression effect, 232
 - thermal, 35, 46
 - non-equilibrium, 158
 - quasi-equilibrium, 158
- particle
 - incident, 9
 - scattered, 9
- probability
 - joint detection, 234
 - single-particle, 215
 - two-particle, 215
- quantized
 - alternating current, 111, 207

- emission regime, 210
- shot noise, 212
- quantum
 - Archimedes screw, 127
 - capacitance, 194
 - inductance, 194
 - pump, 111
 - pump effect, 111
 - existence condition, 115, 119
 - quantized emission regime, 111
- reflection probability, 22
- resistance
 - differential, 198
 - relaxation
 - quantum, 181
- scattering channel, 21
 - dynamic, 109
- scattering matrix, 3
 - anomalous, 83, 133
 - double-barrier potential, 104
 - point-like potential, 91
 - dimension
 - 1×1 , 21
 - 2×2 , 22
 - 3×3 , 23
 - double-barrier potential, 102
 - dual, 84
 - Floquet, 71
 - chiral ring, 182
 - frozen, 78
 - point-like potential, 90
 - spectral current density, 132
 - partial, 132
 - transmission probability, 23
 - two-particle
 - correlation function
 - correlated particles, 236
 - uncorrelated particles, 235
 - correlations, 233